# Chapter 3
# Environmental Effects

## Environmental Stress Cracking (ESC) of ABS (II)

**Takafumi Kawaguchi, Hiroyuki Nishimura, and Fumiaki Miwa**
*Osaka Gas Co.,Ltd., Japan*
**Takashi Kuriyama, and Ikuo Narisawa**
*Yamagata University, Japan*

### INTRODUCTION

It has been known that plastics fail even under very low stress when they are in contact with particular chemical agents. This phenomenon is called environmental stress cracking (ESC). ESC is of great importance in materials selection, because it sometimes becomes the cause of failure in actual use of plastic parts. Woshinis and Wright investigated the cases of many failure cases of plastic parts and they concluded that about one-third of the plastic parts failures were caused by ESC.[1] In particular, outer parts more frequently come into contact with many kinds of agents. The evaluation of the resistance of plastics to ESC is, therefore, important in material selection of outer parts.

For the material of outer parts, acrylonitrile-butadiene-styrene (ABS) co-polymer is widely used because of its favorable cost/performance ratio, luster, and resistance to impact. There are some reports on the ESC of ABS. They have shown that some kinds of chemical agents such as organic solvents and surfactants cause ESC of ABS.[2,3]

The authors investigated the mechanism of the crack propagation of ABS in non-ionic surfactants by ECT tests and a transmission electron microscope (TEM), and reported that the level of local stress at the crack tip was the dominant factor which determined the mechanism of crack propagation.[4,5] It was found in the study that when the local stress at the crack tip was low, a small massive crazed zone originated from the penetration of a non-ionic surfactant and a crack propagated by ESC. As the local stress ahead of the pre-crack tip was relatively high, the toughening mechanism due to the deformation of the rubber particles and the crazing acted ahead of the crack tip and resulted in the arrest of crack propagation.

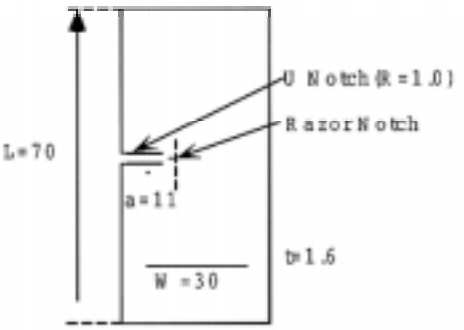


Figure 1. The shape of the specimen for ECT tests.

In this study, the dependence of the ESC of ABS on temperature and on the kind of surfactant was investigated by ECT tests. The fracture surfaces of the specimens in these tests were investigated by a scanning electron microscope (SEM).

## EXPERIMENTAL

### MATERIALS AND SURFACTANTS

The material used in this study was obtained from Ube Saikon Co., Ltd. Two types of non-ionic surfactant (surfactants A and B) were used in this study. One was a kind of poly-oxyethylenealkylphenyllether and the other was a kind of polyoxyethylenealkylether. Their molecular structures are shown below.

Surfactant A: 4-$C_8H_7C_6H_4(OCH_2CH_2)_{12}OH$

Surfactant B: $C_{12}H_{25}(OCH_2CH_2)_4OH$

### ECT TESTS AND SEM

ECT tests were performed under constant loading conditions. Crack length was measured by a CCD camera. The ECT tests were performed in non-ionic surfactants, and the temperatures of the specimens and the surfactants were kept constant (23°C or 50°C) during the tests. Figure 1 shows the shape of the specimens used in the ECT tests. They were cut out from compression-molded sheets. The fracture surfaces of the specimens in ECT tests were observed by a Hitachi SEM S-530 at an acceleration voltage of 20 kV.

## RESULTS AND DISCUSSION

### OBSERVATION OF CRACK PROPAGATION BEHAVIOR IN ECT TESTS

Figures 2 and 3 show the result of an ECT test performed in surfactant A for $\sigma = 8.2 \times 10^5$ Pa at 23°C and 50 °C, respectively. The x-axis denotes time after the initiation of crack propagation and the y-axis denotes crack length.

In Figure 2, it is seen that the curve of crack length can be divided into three regions (regions A, B, and C). In region A, crack propagation began after an incubation time. The whitening zone ahead of the crack tip could not be recognized by a CCD camera. In region B, crack propagation stopped. In this region, the whitening zone ahead of the crack tip was rather large and it could be recognized by a CCD camera. Following this, the crack propagated with a repetition of region A and region B, and in the end, ultimate failure occurred (region C).

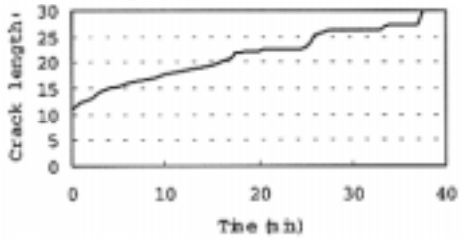


Figure 2. The ECT test result in surfactant A for $\sigma$ = 8.2 x $10^5$ Pa at 23$^o$C.

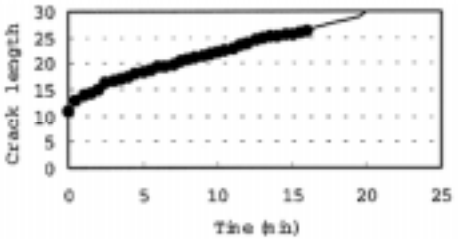


Figure 3. The ECT test result in surfactant A for $\sigma$ = 8.2 x $10^5$ Pa at 50$^o$C.

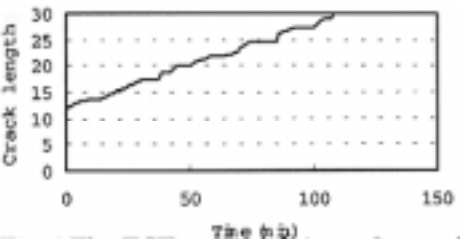


Figure 4. The ECT test result in surfactant B for $\sigma$ = 8.2 x $10^5$ Pa at 23$^o$C.

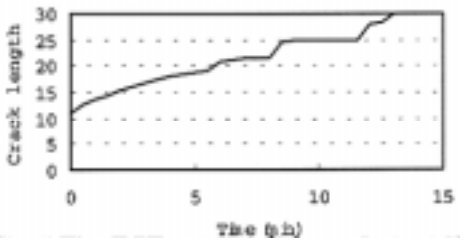


Figure 5. The ECT test result in surfactant B for $\sigma$ = 8.2 x $10^5$ Pa at 50$^o$C.

The behavior of crack propagation shown in Figure 3 was quite different from that in Figure 2. In the initial stage of the test, the crack propagation rate was nearly constant and the arrest of crack propagation was not observed. At a crack length of about 25 mm, the crack propagation stopped and the whitening zone ahead of the crack tip was observed. The total time to failure was rather short compared with that in Figure 2.

Figures 4 and 5 show the results of an ECT test performed in surfactant B for $\sigma$ = 8.2 x 105 Pa at 23$^o$C and 50 °C, respectively. Although the total time to failure was also much shorter when tested at a higher temperature (Figure 5), the crack propagation behavior was similar between the results tested at different temperatures. It was also found that surfactant B gave shorter total time to failure than surfactant A. From these results, it was expected that the penetration of surfactant A into the materials was not so active as that of surfactant B.

Figure 6 shows the SEM image of the fracture surface of the ECT test shown in Figure 2. The crack propagation direction is shown by arrows. In Figure 6, the fracture surface near the pre-crack is flat and it indicates that the crack propagated by ESC. This flat area corresponds to region A in Figure 2. In region B, the local stress at the crack tip was higher than that in region A, and there were several areas which had rougher structures than that in

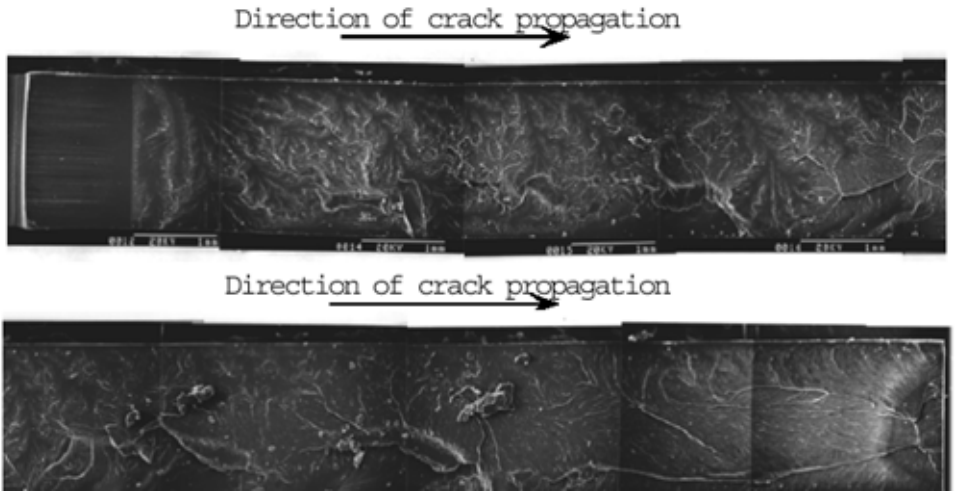


Figure 6. The SEM image of the fracture surface of the ECT test shown in Figure 2.

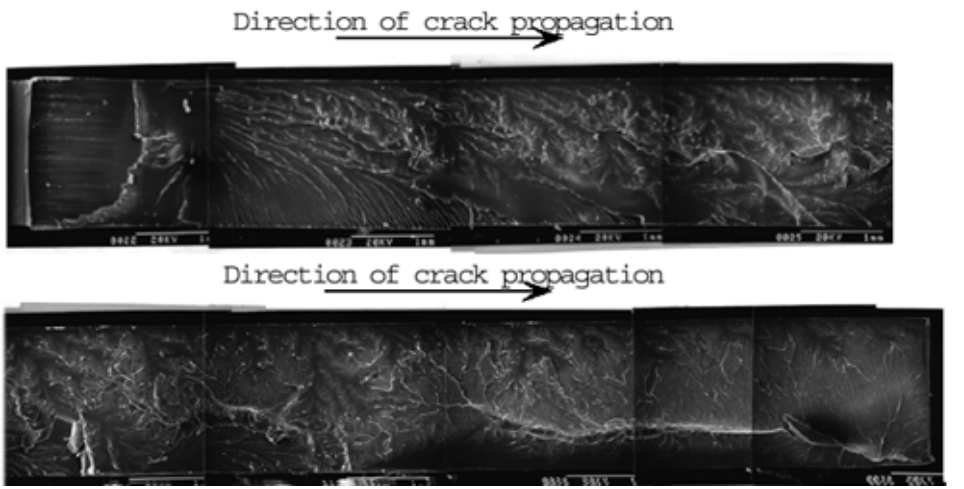


Figure 7. The SEM image of the fracture surface of the ECT test shown in Figure 3.

region A. The rough areas seemed to be the trace of the whitening zone observed in the ECT test, and these areas corresponded to the point of the arrest of crack propagation in the ECT test. The fracture surface of region C was rather rough and it indicated that the specimen fractured in that region mainly by stress.

It was found from these results that the change of morphology of the fracture surface of the ECT specimen corresponded to the behavior of the crack propagation in the ECT test.

Figure 7 shows the SEM image of the fracture surface of the ECT test shown in Figure 3. In Figure 7, the flat area is relatively wide and it corresponds to the fact that in the ECT test, the arrest of the crack propagation was not observed until the crack length was long enough.

## DEPENDENCE OF CRACK PROPAGATION BEHAVIOR ON TEMPERATURE AND ON THE KIND OF SURFACTANT

From these results, it was found that the rise of temperature had different effects on different surfactants. For the case of surfactant B, the rise of temperature had the effect not only of shortening the total time to failure but also of changing the mode of crack propagation. The rise of temperature caused the specimen to be more liable to rupture by ESC without the arrest of crack propagation caused by the change of morphology at the crack tip.

On the other hand, for the case of surfactant A, which gave longer total time to failure than surfactant B, the rise of temperature had the effect of shortening the total time to failure but the crack propagation behavior did not change very much.

As described above, the authors reported the mechanism of the ESC of ABS, which was investigated by ECT tests and a TEM. The crack propagation mechanism is shown schematically in Figure 8. These studies revealed that when the local stress at the crack tip was low in the initial step of the ESC of ABS, a small massive crazed zone originated by the penetration of the non-ionic surfactant. As the local stress ahead of the crack tip was relatively high because of the crack growth, the toughening due to the deformation of the rubber particles and the crazing occurred ahead of the crack tip and resulted in the arrest of crack propagation. The structure of the damaged zone ahead of the crack tip was similar to that of PA/PPO alloy, which indicated that shear banding and crazing coexited.[6]

Figure 8. Schematics of crack propagation mechanism in ECT tests. (a) shows the craze in small area at the crack tip and (b) shows the craze and the deformation of the rubber particles in large area at the crack tip.

From the results of this study, it is suggested that the change of morphology at the crack tip was also affected by the penetration of the surfactant and the crack propagation rate. When the crack propagation rate was high and the penetration of the surfactant was not very active, the morphology change shown in Figure 8(a) tended to appear. On the other hand, when the crack propagation rate was low and the penetration of the surfactant was active, the morphology change shown in Figure 8(b) tended to appear.

The results of this study can be understood from the mechanism of crack propagation explained above. When the temperature was low, the crack propagation rate was low and the specimens were more likely to have the morphology shown in Figure 8(b), and it resulted in the arrest of crack propagation shown in Figures 2 and 4.

When the temperature was high, the rise of temperature had different effects on surfactants A and B. For the case of surfactant A, the penetration of the surfactant was not very active, and the crack propagated mainly with the change of morphology shown in Figure 8(a). For the case of surfactant B, the penetration of the surfactant was more active, and the crack propagated with the change of morphology shown in Figures 8(a) and (b).

## CONCLUSIONS

Environmental stress cracking (ESC) of acrylonitrile-butadiene-styrene (ABS) copolymer caused by two kinds of non-ionic surfactants was studied by edge crack tension (ECT) tests. The dependence of the ESC on temperature and on the kind of surfactant was investigated. The fracture surfaces were investigated by a scanning electron microscope (SEM). It was found that when the temperature was low, the crack propagated by ESC and successive arrest of crack propagation which was caused by the change of morphology in large area at the crack tip. It was also found that when the temperature was high, the rise of temperature had a different effect on each surfactant. In that case, the penetration of the surfactant into the specimen was active, and the crack propagation behavior was almost the same as that at low temperature. On the other hand, if the penetration of the surfactant into the specimen was not so active, the crack propagated mainly by ESC.

## REFERENCES

1 W. A. Woshinis and D. C. Wright, *Adv. Mat. Proc*., 1994, vol **12**, p 39.
2 D. L. Faulkner, *Polymer Eng. Sci*., 1984, vol **24**, p 1174.
3 R. P. Kambour and A. F. Yee, *Polymer Eng. Sci*., 1981, vol **21**, p 218.
4 T. Kawaguchi et al., ANTEC '98, p3175.
5 T. Kawaguchi et al., *J. Polym. Eng. & Sci*. (in press).
6 H-J. Sue and A. F. Yee, *J. Mat. Sci*., 1989, vol **24**, 1447.

# Residual Stress Development in Marine Coatings Under Simulated Service Conditions

**Gu Yan & J R White**
*University of Newcastle upon Tyne, UK*

## INTRODUCTION

Polymer coatings are used extensively for corrosion protection of metals in marine environments. Solvent loss and, in the case of thermosets, the curing process, causes shrinkage of the coating. When it is applied to a stiff substrate the shrinkage in the plane of the coating is resisted and bi-axial tensile residual stresses form. If application of the coating is made at a temperature different from the subsequent service temperature then there will be further residual stresses that result from differential thermal expansion of the coating and substrate. The coating will always have a greater thermal expansion coefficient than the substrate so if the service temperature is less than the application temperature there will be a further increment of tensile residual stress from this source. The stresses may lead to failure of the coating by causing it to crack or to detach from the substrate (flaking, de-lamination, blistering etc.). It is therefore important to have methods to measure the level of residual stress so that its contribution to failure may be assessed.

If the substrate is thin and if the coating is applied to one side only then the tensile stress in the coating causes the coating-substrate combination to bend to restore moment equilibrium, with the coating side becoming concave. The severity of the curvature depends on the level of stress. The most common experimental method of measuring the residual stress in coatings uses a measurement of the curvature, from which the stress can be computed provided that the thicknesses and Young's moduli of the two components are known. In the research described here this approach was used and the behavior of a thermoplastic coating and a thermoset coating were compared during solvent evaporation/curing. The curvature was measured using a strain gauge, permitting continuous monitoring. The method was further extended to examine the changes in residual stress when the coating was submerged in water and when it was removed again to dry out. The coatings formed the basis of an experimental undercoat-top coat system of the kind commonly used in marine applications and measurements were also made on bi-layers.

## EXPERIMENTAL

### SAMPLE PREPARATION

The coatings used here were experimental materials designed for marine applications. The thermoplastic, coded "Anticorrosive A" (or "AA" from now on) was a single mixture containing a vinyl copolymer, solvent (xylene), tar pitch, pigments (57% solids by weight, 38% solids by volume). The thermoset was a two-component system, prepared just before application as with any common commercial two-pack epoxy, and was coded "Anticorrosive B" (or "AB"). AB also contained hydrocarbon resin and pigment and the solvent was Shellsol A. The coating thickness was computed from the mass of the coating after the solvent had disappeared and the density of the solid residue.

The coatings were applied to thin steel shim substrates, chosen because the coatings were designed for marine applications on steel structures. Substrates 100, 150, 200 and 250 $\mu$m thick were used both to determine the best value and as a check on the reproducibility of the residual stress measurements. The shim was cut into coupons 150 mm x 25 mm. Surfaces were prepared for coating and for strain gauge attachment using emery papers #120, #500 and #800 and finally cleaned using acetone or xylene.

A strain gauge was attached to the side of the substrate that was to become the uncoated side using a cyanoacrylate adhesive. A microcrystalline wax coating (M-Coat W-1) was applied over the strain gauge and lead connections to water proof them and permit operation when submerged in water. The substrates were held flat on a magnetic table and the coating applied by hand brush. The coatings were suitable for spraying but spray equipment was not available that could be used in or near to the laboratory in which the subsequent measurements were conducted. The coatings were allowed to dry or cure in a room held at $30\pm1^{o}$C and the strain gauge signal was monitored continuously. Solvent evaporation was normally monitored for 14 days after which time the changes recorded in curvature or mass were minimal in AA. Thus samples for investigation of the effect of water immersion or for overcoating with AB were dried for 14 days before the next phase of the experiment.

### WET/DRY CYCLING

Coated substrates with strain gauges attached to the uncoated surface were placed in an empty tank in a room at $30\pm1^{o}$C then submerged in distilled water at $30^{o}$C, taking care not to disturb the strain gauge reading during filling. The strain gauge signal was monitored for 24 hours or 48 hours then the tank was emptied carefully. The strain gauge reading was monitored for a drying out period equal to the initial immersion period then the cycle was repeated.

## TEMPERATURE CYCLING

Tests were conducted with the samples immersed in water at 5$^{o}$C then at 30$^{o}$C using a 48 hour dwell time.

## EVAPORATION KINETICS

The solvent evaporation kinetics of the coatings were investigated by measuring the weight changes on specially prepared substrates without strain gauges attached. The coating was applied and the first weighing made as rapidly as possible in a Mettler AT analytical balance measuring to 100 $\mu$g. Readings were then taken every 10 seconds for the first 10 minutes then at increasingly long intervals. Measurements were continued for 14 days.

## ABSORPTION/DESORPTION KINETICS

The samples used for the study of evaporation kinetics were then used to investigate the absorption and desorption of water. During absorption, the samples were immersed in water and removed periodically for weighing. Each time they were removed the surface water was removed with blotting paper, they were weighed, then returned to the immersion tank as rapidly as possible. At the end of 48 hours they were removed from the tank, the surface water removed and they were allowed to dry out in room air, taking weighings periodically. After 48 hours of drying out the samples were re-immersed and the cycle repeated.

## YOUNG'S MODULUS OF THE COATINGS

To calculate the residual stress from the curvature of the film plus substrate requires knowledge of the Young's modulus of the coatings. This was measured using tensile tests conducted on dog-bone shaped samples cut from free films of AA and AB. Measurements were made on samples as follows: (a) as-prepared; (b) after immersion in water for 6 days at 30$^{o}$C; (c) after immersion in water for 5 days then dried out for 1 day at 30$^{o}$C; and (d) after immersion in water for 3 days then dried out for 3 days at 30$^{o}$C. The Young's modulus was calculated from the small strain part of the load-deformation curve, which was fairly linear. For the combinations of coating and substrate thicknesses used in this work the Young's modulus is not very critical in the measurement of residual stress.

## CALCULATION OF RESIDUAL STRESS

The residual stress in the coating was calculated using an elastic analysis that assumed that the curvature was spherical, that is that the curvature transverse to the coupon axis was equal to that measured along the coupon axis. The analysis was basically that described by Corcoran.[1,2]

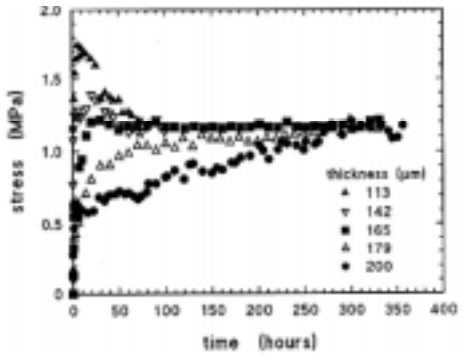


Figure 1. Development of residual stresses during solvent evaporation in AA coatings of different thickness.

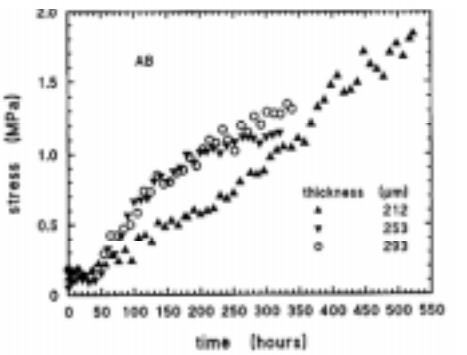


Figure 2. Development of residual stresses during solvent evaporation in AB coatings of different thickness.

## RESULTS

### RESIDUAL STRESSES DURING SOLVENT EVAPORATION

Figures 1 and 2 show measurements of the residual stresses in coatings of different thickness for periods of 14 days or more. The stress in AA coatings of thicknesses ranging between 113 μm to 200 μm converges to a common value of approximately 1.2 MPa after about 12 days (Figure 1). The coatings with thicknesses below 150 μm display a stress maximum (of nearly 1.8 MPa for the thinnest) at short times (<10 hours) before decaying to the common value. For coatings thicker than 150 μm the rate of approach to the final stress value is progressively slower as the thickness is increased. With AB the stress built up most rapidly in the thickest coatings but appeared to be approaching a constant value after 14 days whereas the stress in the thinnest coating (212 μm) was still climbing after 21 days (Figure 2).

The mass loss measurements showed a three stage process. The first stage is free surface evaporation, followed by a mixed kinetics stage, and finally diffusion controlled evaporation.[2] Since solidification does not proceed uniformly across the coating some stress build up occurred due to solidification near the edges while the mass loss characteristic was still in the first stage.[2] This effect was greater in AA than in AB.[2]

### RESIDUAL STRESSES DURING WET/DRY CYCLING

Figure 3 shows the variation in residual stress in AA during wet/dry cycling with a period of 48 hours (that is 24 hours water immersion followed by 24 hours drying out in a room at 30°C). The stress increased rapidly to about 0.4 MPa during the first 2 hours of water immersion then increased much more slowly during the remainder of the first immersion

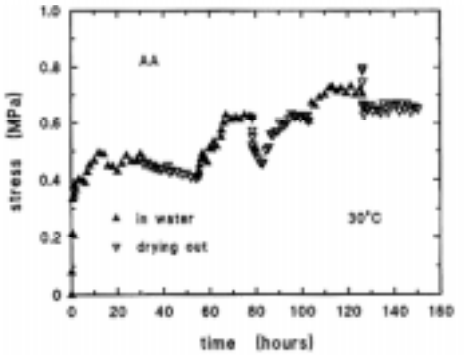


Figure 3. Development of residual stress in an AA coating 165 μm thick during wet/dry cycling at 30°C (48 h period).

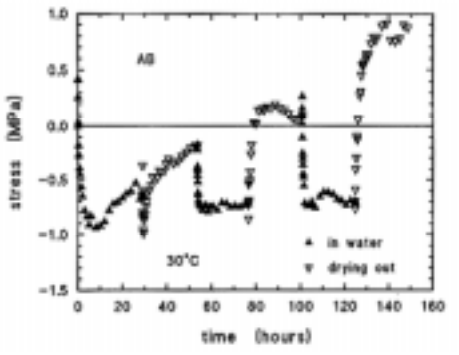


Figure 4. Development of residual stress in an AB coating 212 μm thick during wet/dry cycling at 30°C (48 h period).

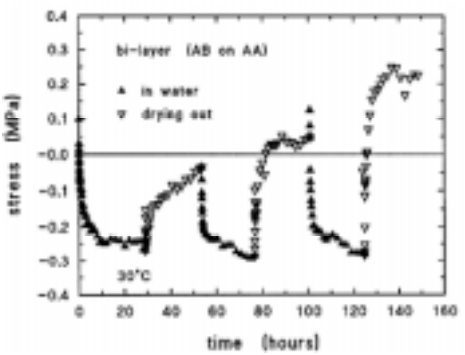


Figure 5. Development of residual stress in a bi-layer coating consisting of 256 μm AB on top of 179 μm AA during wet/dry cycling at 30°C (48 h period).

period. Some reduction of stress was observed during the following drying out period. For subsequent cycles the changes were more modest, but for each complete cycle the increase obtained during immersion was greater than the drop obtained during drying out. It is notable that the stresses recorded are all tensile: if the major effect were swelling of the coating by the uptake of water then the stress would have been compressive and the curvatures would have.been in the opposite sense.

The stress observed in AB was also tensile immediately after immersion (Figure 4) but it quickly reversed to become compressive within half an hour (see reference (2) for a presentation of the results with an expanded time scale). After a compressive minimum of about 1 MPa the stress magnitude in this coating (212 μm thick) reduced for the remainder of the period of water immersion. On removing the water from the tank a further increment of compressive stress was observed but this was quickly reversed and at the end of the first dry period the stress was only slightly compressive. Further wet/dry cycles gave a compressive increment during the wet period followed by a larger tensile increment on drying out so that the net effect was a drift towards tensile

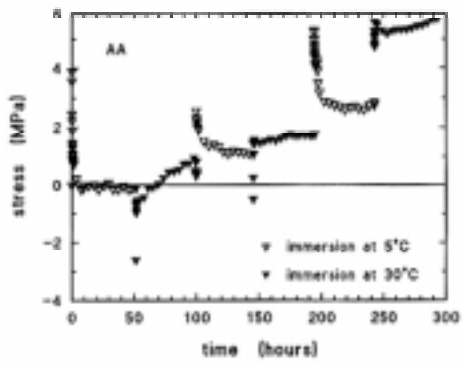


Figure 6. Development of residual stress in an AA coating 252 μm thick during wet (5°C)/dry (room temperature) cycling (96 h period).

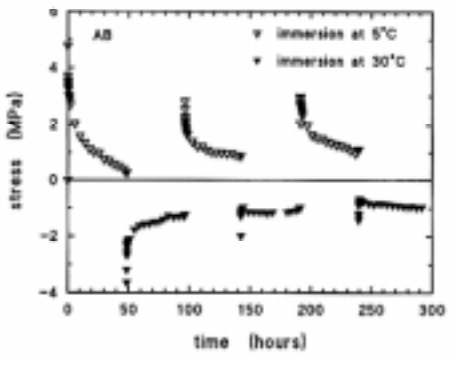


Figure 7. Development of residual stress in an AB coating 235 μm thick during wet (5°C)/dry (room temperature) cycling (96 h period).

stresses (Figure 4). The amplitude of change observed during a cycle increased progressively.

Results similar to those for AB are shown in Figure 5 for a bi-layer of 256 μm AB over 179 μm AA. The main difference between Figures 4 and 5 is the stress scale, which is expanded for Figure 5. Note that for the bi-layers it is assumed that the application of the AB top coat does not change the characteristics of the AA and that the change in curvature of the AB+AA+substrate combination is caused by stress changes in the top coat only. Changes in stress in AA caused by absorption of solvent from AB are ignored. Detailed differences occurred in the stresses observed for different coating thicknesses and, for bi-layers, different combinations of coating thicknesses.[2] Tensile stresses of nearly 2 MPa were observed during the drying out phase of the second and third cycle of an AB coating 293 μm thick. In bi-layers the stress after several cycles depended on the relative thickness of the two components and could be either tensile (generally when AA thickness was greater) or compressive (generally when AB thickness was greater).[2]

## TEMPERATURE CYCLING

Cooling samples to 5°C produced large tensile stresses which relaxed significantly during the cold dwell (Figures 6-8). In AB the stress reversed on returning to 30°C and the stress changes were repeated each temperature cycle (Figure 7). In the AA coating there was a progressive drift to higher (tensile) stresses (Figure 6). Bi-layers showed behavior closer to AB than to AA (Figure 8).

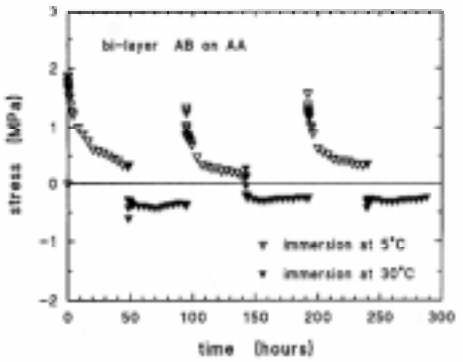


Figure 8. Development of residual stress in a bi-layer coating consisting of 264 μm of AB on top of 142 μm of AA during wet (5°C)/dry (room temperature) cycling (96 h period).

## DISCUSSION

The residual stress development in AA coatings was similar to that observed by Croll[3,4] who also found that the residual stress in thermoplastic coatings reached an equilibrium value that was independent of the thickness and that the thickest coatings took the longest time to reach equilibrium. Tensile stresses form as the result of the volumetric shrinkage that accompanies the loss of solvent. During the early part of this process the coating is still fluid and stresses begin to form only when sufficient solvent has been lost for the coating to develop some energy elastic resistance to deformation. The time dependence of stress build up is determined by the diffusion of solvent through the coating and by the relaxation processes in the coating. The concentration profile will be dependent on the coating thickness and the relaxation rate will depend on the concentration. It is thus curious that the final stress level should be independent of coating thickness.

The residual stresses in AB thermoset coatings were also tensile but showed greater scatter in magnitude and did not always approach a steady value even after 22 days. Croll[5] also investigated thermoset coatings but used a solventless amine-cured epoxy. In his studies the coatings developed compressive stresses when thin (<55 μm, thinner than any of the coatings investigated in the current work) and tensile stresses when in the range of thicknesses used here. Croll could not use solvent evaporation to explain stress development and he attributed the tensile stress to structural changes during the curing process. He surmised that compressive stresses were caused by swelling due to water absorption (from the atmosphere). No attempt was made to control the humidity in the experiments reported here and the small lack of consistency between different runs with AB coatings may have been caused by different contributions from this source. In the case of thermoset coatings the diffusion of solvent becomes progressively more difficult as the polymer network develops and release of solvent may proceed for an extended period of time.

When AB was overcoated on top of a dry AA coating, solvent release from AB was not only into the air at the free surface but also into AA at the interface between the two coatings. Solvent entering AA will cause swelling giving an increment of compressive stress so that the overall build up of stress was much slower than for a similar AB coating applied

direct to the substrate and the increment of stress due to the AB coating was much less than that obtained with an AB coating alone.[2]

The behavior of the coatings when immersed in water and on subsequent drying out requires careful consideration. The initial tensile stress observed in AA coatings has not been explained with certainty. It is speculated that water may plasticize the coating, assisting the escape of residual solvent (or some other minor component). Subsequent changes in stress on dry/wet cycling are small but the sense of the changes are opposite to those which would be caused by water swelling during immersion and reversal of this effect during drying out. It is as if water has occupied the free volume and provided attractive forces to draw the molecules closer together. After water immersion the measured Young's modulus of AA was higher than after solvent evaporation and it increased still further if allowed to dry out partially. This could be explained if water acted both to plasticize the polymer and to provide stronger intermolecular bonds and if the water participating in plasticization was less tightly bound (and more easily lost on drying out) than that providing intermolecular bonding.

An initial increment of tensile stress was also observed in AB coatings on water immersion, possibly caused by a similar mechanism to that in AA. After about half an hour this effect reversed and subsequently for all phases of the wet/dry cycling the changes in stress were consistent with swelling by water (giving compression) with reversal during desorption of water. The overall drift in stress in the tensile direction could be due to further solvent evaporation (assisted by water plasticization of the coating). Broadly similar results were obtained by Negele and Funke[6] using a simpler epoxy coating.

Of perhaps greatest interest here are the results obtained with AB coatings on top of AA coatings. The results are explainable qualitatively in terms of water diffusing through the AB coating and on into the AA coating during immersion and then this process reversing during drying out. The concentration gradients will be complex and will cause significant inertia in the time signature of the changes. As a result of the different stress responses of AA and AB coatings to water the sense of stress in the bi-layer coatings depended on the relative thickness of the two layers, with smallest stresses occurring when their thicknesses were approximately equal.

The largest stresses were obtained during the temperature cycling experiments. Differential thermal contraction is believed to be responsible for the generation of tensile stresses of the order of 4MPa in AB coatings on immersion into water at $5^{o}$C. Partial relaxation of this stress then occurred and this caused the formation of compressive stress when the sample was restored to a higher temperature. The behavior of AA was basically similar but with a drift towards a permanent tensile stress. AB on top of AA showed behavior similar to that of AB.

## CONCLUSIONS

The highest residual stresses observed in this study were caused by differential thermal contraction between coating and substrate. A temperature change similar to that between a dry dock in a warm climate and the open sea gave stresses of 4 MPa and more, a significant fraction of the failure strength. Other sources of residual stress are complex and are probably highly specific to the coating composition. When using bi-layered coatings the changes in stresses were moderated somewhat and it appears that a significant and beneficial reduction in the stress magnitude can be achieved by appropriate combination of thicknesses of the two layers.

## ACKNOWLEDGEMENTS

The authors acknowledge Courtaulds Coatings for providing the materials used in this study and for the provision of a strain gauge signal conditioning unit. We are grateful to M Buhaenko for advice and for stimulating discussions throughout the project.

## REFERENCES

1 E M Corcoran, *J.Paint Technol*., **41** (1969) 635
2 Yan Gu, MPhil thesis, University of Newcastle upon Tyne (1997)
3 S G Croll, *J.Coatings Technol*., **50 (638)** (1978) 33
4 S G Croll, *J.Appl.Polym.Sci*., **23** (1979) 847
5 S G Croll, *J.Coatings Technol*., **51 (659)** (1979) 49

# Estimation of Long-term Properties of Epoxies in Body Fluids

**Steven W. Bradley**
*Materials Performance, Inc., College Station, TX, USA*

## INTRODUCTION

The selection of materials for use in the human body often requires unique evaluation techniques. Beyond the normal toxicological and tissue rejection considerations, the saline body fluid environment, elevated temperature (37°C) and complex stress loadings must be considered. In this work, two candidate epoxies were evaluated for the attachment of two polysulfone lumens. Both candidates displayed adequate strength under dry room temperature loading. The preferred candidate material was selected for ease of use as a room temperature cure epoxy. However, the material had a potentially low glass transition temperature, $T_g$. A course of investigation was as follows: (1) perform an extensive literature review to determine what the potential effects of moisture were on the adhesive strength, cohesive strength and $T_g$ of the candidate epoxies, (2) compare glass transition temperatures of moisture saturated versus dry candidate materials and (3) establish a protocol using master curves for the accelerated performance evaluation of candidate epoxies.

## THEORY OF MOISTURE EFFECTS

Absorbed moisture may degrade an epoxy adhesive in at least four ways: (1) reduction in interfacial adhesion; (2) reduction of the cohesive strength of the adhesive due to plasticization; (3) reduction in the glass transition temperature; and (4) swelling which produces local residual stresses which can be significant.

## REDUCTION IN INTERFACIAL ADHESION

Previous work[1-3] addressed the effect of moisture on epoxy adhesives used in conjunction with metals which found that soaking and subsequent testing generally produced reductions in strength of less than 50%. Continuous loading or stress in a moist environment generally produced even greater reductions in creep rupture strength at times of one year or longer, with values of 80-90% reported in some cases.[1] Previous work[4,5] alluded to good interfacial bonding between a DGEBA/DDS epoxy system and polysulfone (PSF), where PSF was a

second toughener in the system. However, the effect of moisture and a more quantitative measure of the interfacial strength between common epoxies and polysulfone were not found in the literature. This appears to be an important area for experimental work to confirm the behavior of epoxy adhesives for PSF, both dry and wet.

## REDUCTION IN COHESIVE STRENGTH

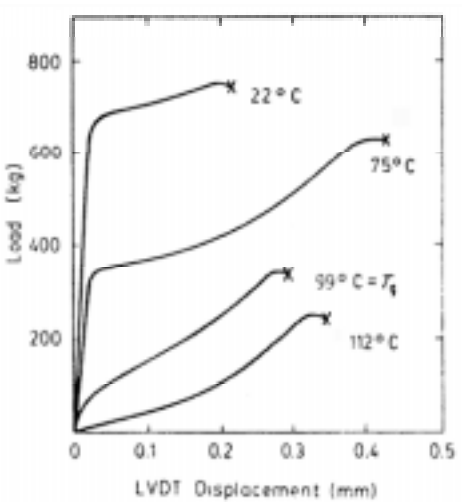


Figure 1. Illustration of loss in strength for an epoxy approaches $T_g$.[2]

Generally the degradation of an epoxy is found to be a reduction in the cohesive strength, though the failure is more often adhesive at higher temperatures. The reason for this behavior can be understood by examining Figure 1,[2] which shows load-displacement behavior for an epoxy which is cured at 121°C and has a $T_g$ = 99°C. Note as the test temperature approaches $T_g$, the materials yield strength drops dramatically. Furthermore, the load supported at $T_g$ would not be possible in anything but a short-tem test. For longer term testing or service loading, the viscoelastic creep of this material would produce a time dependent failure at a very small load. Generally, a lower cure temperature gives a lower $T_g$ and moisture shifts the $T_g$ to a value 10-40°C lower than the dry $T_g$. Thus, an epoxy adhesive with a moderate cure temperature, saturated in water, can have a $T_g$ that is very near room temperature, giving essentially zero yield strength at room temperature and about the same creep rupture strength for longer term applications. Sharon et. al.[6] provide a summary of both the variation of $T_g$ with moisture content and the effect of service/test temperature relative to $T_g$ in determining mechanical properties. It is important to keep in mind that the mechanical properties given[6] are short term tensile properties. Establishing an operating temperature for longer term service relative to $T_g$ would be different (and much lower relative to $T_g$) than what one would infer from these results.

## REDUCTION IN GLASS TRANSITION TEMPERATURE

Previous authors[6-10] give examples of moisture absorption by epoxy resins and the consequent effect on the glass transition temperature, $T_g$. Moisture absorption ranges from 2.4% to greater than 5% by weight, with greater moisture absorption at higher temperatures and

for crosslinking agents that are more hydrophilic. The effect of saline body fluids (0.9% salt) appears to be similar to seawater where the salt water has been found to be absorbed at a slightly lower rate, with presumably the salt not being readily absorbed. A lowering of $T_g$ by 10-40°C had been noted due to absorbed moisture.[6] Thus, the initial $T_g$ (dry) needs to be sufficiently high so that the wet $T_g$ exceeds the service temperature by >50°C for long term, continuous load applications. If a $T_g$ shift of 40°C due to absorbed moisture is possible and a service temperature of 37°C is envisioned, then a dry $T_g$ of 37+40+50=127°C would be prudent.

## SWELLING INDUCED STRESSES

Moisture induced swelling can produce significant residual stresses in a part. The actual magnitude depends on both the amount of moisture absorbed, its distribution, and the degree of constraint provided by the system. If, for example, the horizontal bond line were to experience swelling, the constraint of a vertical bond line would result in the development of residual stresses along the vertical portion of the bond line loaded in shear. These stresses might be significant relative to those produced by the service loads. Again, measured swelling strains in combination with analysis can answer such questions.

## EXPERIMENTAL & RESULTS

### DETERMINATION OF GLASS TRANSITION TEMPERATURE

Samples of both epoxies were placed in 0.9% saline solution that simulated body fluid. The fluid saturation of the sample was measured by comparing the initial weight of the epoxy with the weight after soaking in solution. On average, the water uptake was 1.5%. The samples were still gaining a small amount of water weight when the tests were performed due to time constraint. The samples were analyzed on a Thermal Analysis 9900 DSC. The materials were heated at a rate of 5, 10, 20°C/min to about 180°C. All results were within 2-3°C of each other. Software was required to determine the $T_g$ as the moisture absorption smoothed the break in the DSC output curve that indicates a glass transition. Several runs were performed for each material to provide for minor differences in curing, saturation or sample size. The results for each epoxy,

**Table 1. Average $T_g$ for two epoxies at dry and saturated conditions**

| Material | Average $T_g$, °C |
|---|---|
| Epoxy A (dry) | 59.5 |
| Epoxy A (sat.) | 48.9 |
| Epoxy B (dry) | 89.8 |
| Epoxy B (sat.) | 82.3 |

both with and without water, are shown in Table 1. Epoxy A had a saturated $T_g$ 10.6°C lower than the dry samples. Epoxy B had a saturated $T_g$ 7.5°C lower than the dry samples. Additional moisture uptake might shift the $T_g$ as much as 15°C.

## USING DYNAMIC MECHANICAL ANALYSIS TO CREATE MASTER CURVES

Dynamic mechanical testing provides information for the storage modulus, loss modulus and phase lag during testing. For a given temperature/frequency sweep, variations in these parameters provide information about molecular relaxation processes occurring in the material. Several peaks may form during a sweep which provide valuable information about the material. The first peak below the melting point is generally known as the "alpha" peak, or the glass transition temperature, $T_g$. The next peak that may appear is commonly known as the "beta" peak that quantifies smaller changes in molecular conformation when a certain activation energy is reached. In the tensile mode, the oscillatory strain is described by:

$$\varepsilon = \varepsilon_o \sin(\omega t) \quad [1]$$

where $\varepsilon_0$ is the strain amplitude and $\omega$ is the angular frequency. The corresponding stress is given by:

$$\sigma = \sigma_o \sin(\omega t + \delta) \quad [2]$$

where $\sigma_0$ is the stress amplitude, $\omega$ is the angular frequency and $\delta$ is the phase lag between the sinusoidal stress and strain curves. The greater the viscosity the greater the phase lag and the higher the elasticity, the smaller the phase lag. For the DMA, the relation between stress and strain is described as:

$$\sigma = \sigma_o E' \sin(\omega t) + E'' \cos(\omega t) \quad [3]$$

where $E'$ and $E''$ are the storage and loss modulus, respectively. The time dependent nature of viscoelastic materials has allowed the development of "master curves" that predict the behavior of polymers far beyond practical testing times. Stress-relaxation curves of a polymer made at different temperatures are superimposed by horizontal shifts along a logarithmic time scale to give a master curve. At temperatures below $T_g$, the free volume is small and $a_T$ is best modeled by the Arrhenius equation:

$$\ln a_T \cong \ln \frac{\eta}{\eta_r} = \frac{E_a}{R}\left(\frac{1}{T} - \frac{1}{T_r}\right) \quad [4]$$

Master curve data was plotted for three different temperatures. All measurements were made at 5 K intervals and thus are at 35°C, 50°C, and 90°C rather than at 37°C for example. The plot at 35°C may be.interpreted as the behavior of the two tested epoxies if kept in a nominally dry condition. The plot at 50°C may be interpreted as the behavior of the epoxies at 37°C with moisture saturation. The 13-degree difference was a result of the plasticization effect of moisture on the epoxy which lowers the $T_g$ as shown in Table 1. The time equiva-

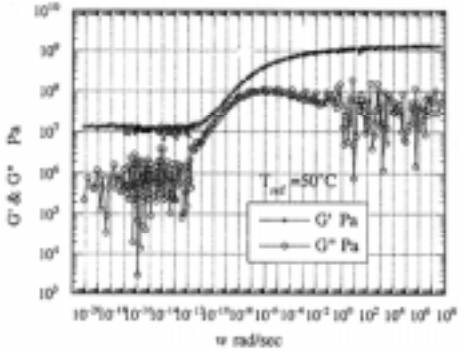


Figure 2. Master curve for Epoxy B at 50ºC.

**Table 2: DMA shear modulus values**

| Material | 15 min modulus, MPa | 1 year modulus, MPa |
|---|---|---|
| Epoxy A (dry) | 700 | 100 |
| Epoxy A (wet) | 300 | 7 |
| Epoxy B (dry) | 900 | 600 |
| Epoxy B (wet) | 700 | 100 |

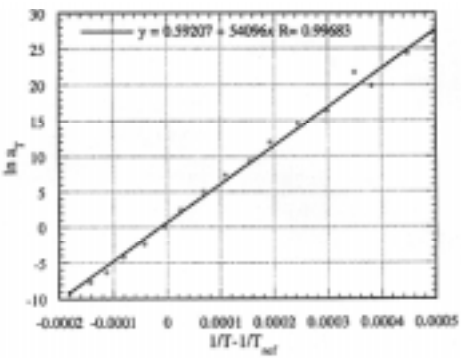


Figure 3. Arrhenius plot for Epoxy B activation energy determination.

lent to a one year test is found in Figure 2 by multiplying the time in seconds by four as the time to load is only ¼ of a cycle. The inverse of this number is the frequency on the plot (8E-9 Hz). A comparison of shear modulus for wet versus dry epoxy as taken from DMA plots at 50°C (wet equivalent) and 35°C (dry) are shown in Table 2. Note that the moisture saturated Epoxy A is completely in the rubbery plateau after one year and would not be useful for bonding purposes. Epoxy B saw a significant modulus reduction due to the proximity to $T_g$ after one year.

A simple calculation can be made using the Arrhenius relationship that would provide the required temperature elevation to represent long term behavior of the material. The Arrhenius relationship requires an activation energy which can be found from the slope of a $\ln a_T$ vs 1/T plot as shown in Figure 3 for Epoxy B. Calculations for Epoxy B using equation 4 indicate that testing dry specimens for 15 minutes at 72°C will give similar behavior to testing specimens for 1 year at 37°C wet, as far as the modulus is concerned. If significant reductions in the modulus are noted, a significant reduction in strength can also be anticipated, in as much as the same molecular motions that give small elastic strains must be observed to allow the deformation processes that ultimately lead to failure. Similar calculations for Epoxy A would require testing at 100°C to indicate the long-term cohesive strength at 37°C, wet. This was far above the glass transi-

tion temperature of 59°C for Epoxy A indicating that the long term behavior prediction by elevated temperature testing for Epoxy A is not possible. This was also indicated further by the nonlinearity of the Arrehenius plot for Epoxy A.

## CONCLUSIONS

Moisture and temperature both act to reduce to strength of epoxy in bodily fluids. Two epoxies were evaluated for adhering polysulfone lumens together. Each material was moisture saturated and then place in a DSC fo $T_g$ determination. The drop in $T_g$ for the two materials was between 7 and 10°C. Further moisture saturation might have produced $T_g$ drops as high as 15°C according to literature. DMA temperature/frequency sweeps were performed at temperature shifts equivalent to the moisture effect on $T_g$. Epoxy A lost more than 97% of its modulus after one year and was in the rubbery region of the modulus plateau. Epoxy B lost 85% of its modulus after the first year. Finally, a calculation using the Arrhenius relationship found that mechanical testing at 72°C for 15 minutes would give some indication of long term cohesive strength at 3°C, wet.

## REFERENCES


1 C.O. Arah, et. al., "The Correlation between Adhesive Stress-relaxation and Joint Performance" *SAMPE Journa*l, Vol. **25**, No. 4, pp. 11-13 (Jul 1989).

2 R.A. Jurf, J. R. Vinson, "Effect of Moisture on the Static and Viscoelastic Shear Properties of Epoxy Adhesives," *Journal of Materials Scienc*e, Vol **20**, pp. 2979-2989 (1985).

3 M.R. Bowditch, D. Hiscok, D. Moth, "Relationship Between Hydrolytic Stability of Adhesive Joints and Equilibrium Water Content," *Int. Journal of Adhesion & Adhesives – Adhesion 9*0, V. **11**, no. 3 (1991).

4 B.G. Min, Z.H. Stachurski, J.H. Hodgkin, "Microstructural Effects and the Toughening of Thermoplastic Modified Epoxy Resins," *Journal of Applied Polymer Scienc*e, Vol. **50**, pp. 1511-1518 (1993).

5 J.L. Hedrick, M.J. Jurek, I. Yilgor, J. McGrath, "Chemical Modification of Matrix Resin Networks with Engineering Thermoplastics. I. Synthesis and Properties of Epoxy Networks Modified with Amine Terminated Poly(Aryl Ether Sulfone) Oligomers," *Polyme*r, V. **32**, no. 11, pp. 2020-2032 (1991).

6 G. Sharon, H. Dodiuk, S. Kenig, "Hygrothermal Properties of Epoxy Film Adhesives," *Journal of Adhesio*n, pp. 87-104 (1989).

7 K. Takahashi, "Mositure instusion in $SiO_2$/Epoxy Interfaces," *Mat. Res. Soc. Symp. Pro*c., Vol. **153**, pp. 187-192 (1989).

8 J. Gorbatkina, N. Shaidurova, "The Effect of Aging in Water on the Strength of Fiber-Polymer Systems," *J. of Adhesio*n, Vol. **35**, pp. 203-215 (1991).

9 J. Comyn, et. al., "Effect of Water on Adhesives & Adhesive Joints," *Plastic Rubber Process App*l, V**3**, n3, pp. 201-205 (1983).

10 C. Ombra, et. al, "Long Term Aging Behaviour of Epoxy Matrices in Aggressive Environments," *Interrelations Between Processing Structure and Properties of Polymeric Material*s, pp. 615-626 (1984).

# Mechanical Performance of Polyamides with Influence of Moisture and Temperature – Accurate Evaluation and Better Understanding

**Nanying Jia and Val A. Kagan**
*Honeywell, Morristown, NJ 07962-1021, USA*

## INTRODUCTION

The plastic industry has no doubt witnessed in recent years an increase in interests and demands in using thermoplastics, such as polyamides, to replace certain metals and thermosets in manufacturing automotive air induction and power train systems, lawn/garden and other power tools. Technologies have also advanced to accommodate these demands by developing materials and products with higher performance, less weight, more time/cost savings, optimized welded joints, and better resistance to fatigue and environmental changes.[1-3]

The important roles today's thermoplastic structures are designed to play have made it increasingly critical for the materials to perform, especially under adversary working and environmental conditions such as cyclic stress/strain, high and low temperatures, and changing humidity.

The short-term and long-term mechanical properties (tensile and fatigue) of polyamide (PA), or nylon, based plastics under dry-as-molded (DAM) conditions were analyzed previously.[1-2] Fatigue properties of unfilled nylon 6 and nylon 66 at room temperature conditions with the influence of absorbed moisture were also discussed.[4] The absorbed moisture (≤2.5 wt%) decreased fatigue crack growth rates, which might reflect the ability of tightly bounded water to enhance chain mobility. Results on combined moisture-temperature effects on short-term and long-term properties of polyamides, on the other hand, were rarely found in the literature.

The current investigation has been focused on the combined effects of moisture-temperature on the short-term (tensile) properties of reinforced nylon 6. Specifics in nylon conditioning using ISO and ASTM procedures are discussed elsewhere.[5] The purpose of this investigation is to help designers of plastic parts and assembled product, material developers, and the database users to correctly interpret the data on tensile properties.

## THE EFFECT OF MOISTURE

Despite its high performance and easy processing, Nylon's tendency and ability of absorbing moisture from the surrounding environment has made it a constant challenge for processing and design engineers alike. The moisture is known to affect a range of polymer properties, which in turn impact processability, dimensional stability, mechanical, acoustic, electrical, optical, and chemical properties, and ultimately the performance of products.[6-7]

The moisture in nylon acts as a plasticizer that reduces the entanglement and bonding between molecules, therefore increases their volume and mobility.[7] The moisturized material exhibits lower glass transition temperature ($T_g$), which makes it easier for further crystallization. The increase in moisture may cause profound changes in a material's behavior under load; it reduces strength, stiffness, and natural frequency, while increasing energy absorption and ductility in the material. Practically, the best way to minimize the moisture uptake is to select plastics with low absorption rate or design products in ways to prevent excessive absorption.

Under dry-as-molded (DAM) conditions, polyamide, or nylon, usually contains 0.1-0.3% water. At room temperature and 50% relative humidity (RH), type 6 polyamide could eventually absorb 2.75% water. Every 1% moisture increase in nylon may result in 0.2 to 0.3% increase in its dimension.[6] This change in dimension would have to be accommodated by preconditioning parts prior to service.

## SAMPLE CONDITIONING – METHOD AND ANALYSIS

Realizing the fact that the properties of dry-as-molded materials often do not reflect their true behavior in service due to the changes in properties caused by the subsequent moisture uptake, sample conditioning is therefore applied to adjust the moisture content in the materials to a desired level so that their properties and performance can be properly tested and analyzed. In this regard, ISO-291 defines the following two standard atmospheres for conditioning:

- "Atmosphere 23": 23/50 (temperature in °C/relative humidity in %) as recommended for most applications;
- "Atmosphere 27": 27/65, as recommended for tropical regions.

For practical purposes it is very important to analyze the properties of thermoplastics conditioned under "Atmosphere 23" (23°C/50%RH), which is recommended for most industrial applications such as automotive, lawn & garden, power tools, appliances, and so on.

The rate of moisture absorption, however, is very low under "Atmosphere 23". In this environment, it would take more than a year for the moisture in an ISO-3167 multipurpose test specimen (4 mm thick) of PA 66 to reach equilibrium. To accelerate this process, one

must increase the conditioning temperature, and/or the relative humidity. Several such conditioning procedures that may be applied to thermoplastics are shown in Table 1.

**Table 1. Methods of Moisture Conditioning for Thermoplastics**

| Standard | Procedure | Use/Comment |
|---|---|---|
| ISO-291; ASTM D618 | Six conditions varying by atmosphere, temperature, water, duration, relative humidity | Standard procedure prior to testing; not a good choice for DAM nylons due to their sensitivity to moisture |
| ISO-62; ASTM D 570 | Water absorption at 23±1°C, 50±1°C, 105-110°C between 0.5 and 24 h. | See Table 2 for data. The moisture at equilibrium varies between 1 to 14% depending on temperature & RH; the microstructure of polymers may be affected by high temperature and high RH (e.g. boiling water). |
| ISO 483; ASTM E 104 | Conditioning done in saturated salt solutions with different RH and temperature. | See Table 3 for results. |
| ISO-1110 | Conditioning performed at 70°C and 62% RH. | Materials tend to “over-saturate” under using this procedure, comparing to the “Atmosphere 23” |

**Table 2. Water absorption values for selected thermoplastics after 24 h. (ISO-62, ASTM D570)[6]**

| Material | Water absorption |
|---|---|
| PP | < 0.01% |
| PC | 0.15% |
| Nylon 11 | 0.25% |
| Nylon 6 | 1.3% |
| Cellulose acetate | 1.7% |

**Table 3. Influence of relative humidity on water absorption in non-filled nylons (at 23°C in air)[7]**

| Type of PA | Relative humidity, % | | | |
|---|---|---|---|---|
| | 30 | 50 | 62 | 100 |
| PA 46 | 1.4 | 3.8 | 5.0 | 15 |
| PA 6 | 1.1 | 2.75 | 3.85 | 9.5 |
| PA 66 | 1.0 | 2.5 | 3.6 | 8.5 |

Table 2 lists the water absorption values for several plastics as determined by ASTM D-570 after 24 h immersion at 23°C. Equilibrium values for water absorption will be significantly higher for these materials. The water absorption will also be higher at elevated temperatures. For unfilled nylon 6, the moisture at equilibrium at 23°C and 50% RH is 2.75% (see Table 3).

Once conditioned, it becomes important for the moisture level to be determined accurately. Moisture analysis for pellets and parts is critical for manufacturing and other processes such as molding, testing, and end-use. Table 3 shows the equilibrium moisture levels at different RH for several commercial nylons, and Table 4 lists several methods of determining moisture for nylon based thermoplastics.

**Table 4. Standard methods of moisture analysis for nylon (PA) thermoplastics**

| Standard | Use/Comment |
|---|---|
| ASTM D789 (Karl-Fischer) | Analysis is based on titration with a Karl Fischer reagent. It is sensitive to moisture from 0.1% to 0.2% with typical sample weight 20 ~ 30 g. Smaller sample size is preferred for higher moisture content |
| ASTM D 4029 | Analysis is based on release of water vapor, which is carried away by an inert gas into an electrolytic cell. It can determine moisture in nylon at a level < 0.1% from a sample 2 ~ 4 g in weight. In a "dry" state the moisture content in nylon based thermoplastics is between 0.05% (nylon 46) and 0.3% (nylon 612) (ASTM D 4066). For nylon 6 the number is ~ 0.2%. |
| ISO-1110, ASTM D 570 | Analysis is based on weight gain. A precision of 0.001 g is required for the weight determining device. |

## MATERIALS AND EXPERIMENTAL PROCEDURES

### MATERIALS

The material used in this investigation was heat-stabilized nylon 6 with 33 wt% glass fiber reinforcement. The material was injection molded into several configurations:

- 4 mm thick ISO multi-purpose tensile bars (ISO-3167);
- 3.2 mm thick ASTM Type I tensile bars (ASTM D638) and ASTM flex bars (ASTM D 790);
- 4 and 6.4 mm thick plaques.

The molded specimens were tightly sealed prior to conditioning and testing in order to preserve their dry-as-molded state while the moisture content remains at ~ 0.2%.

## PROCEDURE FOR MOISTURE CONDITIONING

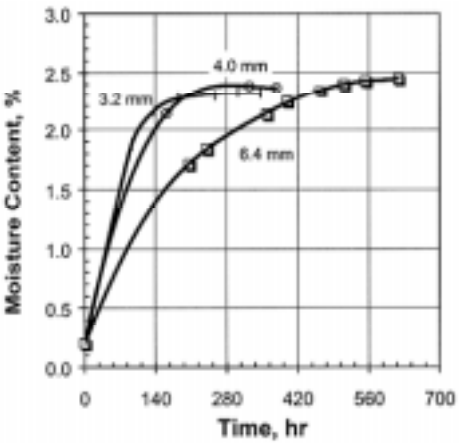


Figure 1. Moisture absorption vs. time for 33% glass fiber reinforced nylon 6. The number in mm by each curve indicates the thickness of the samples.[5]

The procedure for sample conditioning was based on ISO-1110. The molded specimens were loaded into an environmental chamber where the temperature and relative humidity were maintained at 70°C and 62%, respectively. The moisture uptake in the sample was periodically calculated by recording the weight gains using a Mettler balance. The water absorption was also determined on a small group of samples using a Karl-Fischer unit. The moisture content in samples with different thickness was plotted against the conditioning time, as shown in Figure 1.

Although the method in ISO-1110 can greatly accelerate the moisture absorption in nylon compared to the standard method such as "Atmosphere 23", prolonged exposure of samples under conditions specified in ISO-1110 (70°C and 62%RH) has been found to cause "over conditioning" in materials by injecting more moisture than what one can ever obtain when conditioned under "Atmosphere 23". For this reason, the conditioning was terminated once the moisture in the material was found to have reached the equilibrium level under "Atmosphere 23". Samples were then sealed tightly in moisture proof bags until tested or analyzed.

## PROCEDURE FOR TENSILE PROPERTY TEST

The tensile properties of reinforced nylon 6 used in this study was obtained by following ISO-527. Tests were conducted on ISO multipurpose specimens using an Instron 4505 universal testing system. Tests at high and low temperatures were conducted in an environmental chamber attached to the Instron frame. During the test, the temperature at the center of the chamber was maintained at ±2°C within the set point. The detailed description of test setup can be found elsewhere.[1-2]

## RESULTS AND DISCUSSIONS

Figures 2a ~ 2c compare the tensile behavior (stress-strain curves) of DAM and moisturized nylon 6 at –40°C, 23°C, and 120°C, temperatures among those typically found in the end-use conditions. Changes in tensile strength, Young's modulus, and strain at yield versus moisture are shown in Figures 3 and 4.

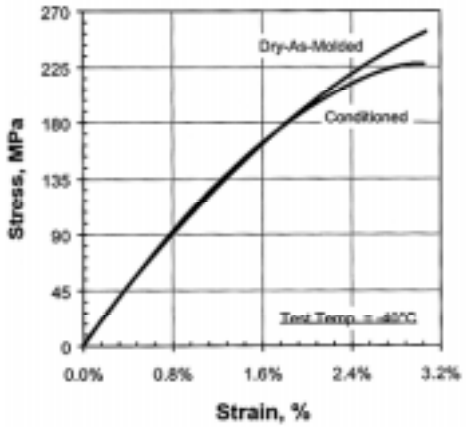


Figure 2a. Effect of moisture on tensile behavior of reinforced nylon 6 (33% glass fiber) at low temperature.

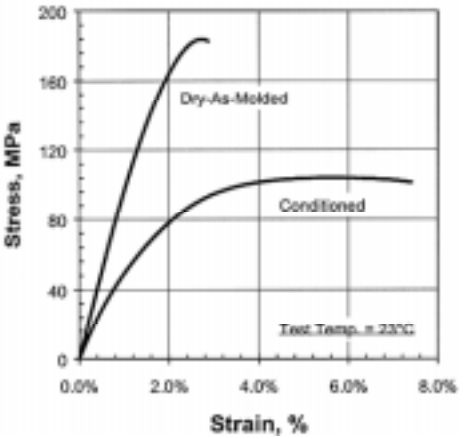


Figure 2b. Effect of moisture on tensile behavior of reinforced nylon 6 (33% glass fiber) at room temperature.

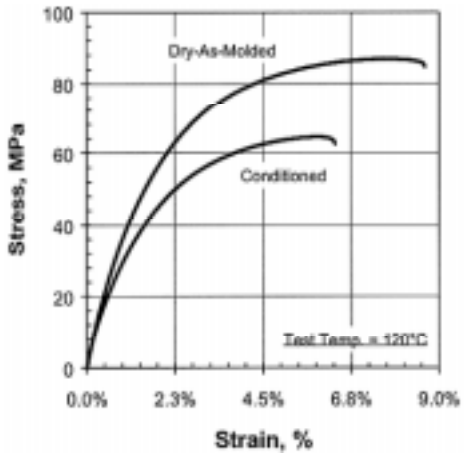


Figure 2c. Effect of moisture on tensile behavior of reinforced nylon 6 (33% glass fiber) at elevated temperature.

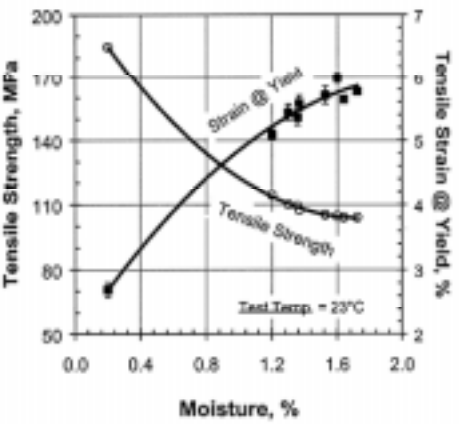


Figure 3. Effect of moisture on tensile properties of reinforced nylon 6 (33% glass fiber); tensile strength and strain at yield vs. moisture at room temperature.

The effect of temperature on tensile behavior can be found in Figures 5a and 5b for DAM and conditioned materials, respectively. The decrease in strength and modulus due to the rising temperature is shown in Figure 6.

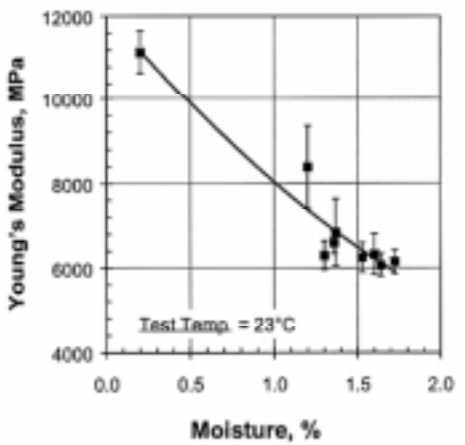


Figure 4. Effect of moisture on Young's modulus: 33% glass fiber reinforced nylon 6.

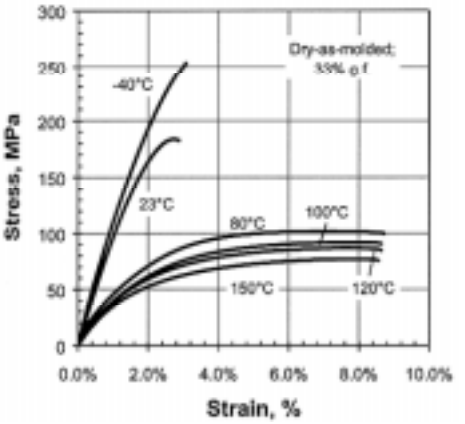


Figure 5a. Effect of temperature on tensile behavior of dry-as-molded nylon 6 (33% glass fiber).

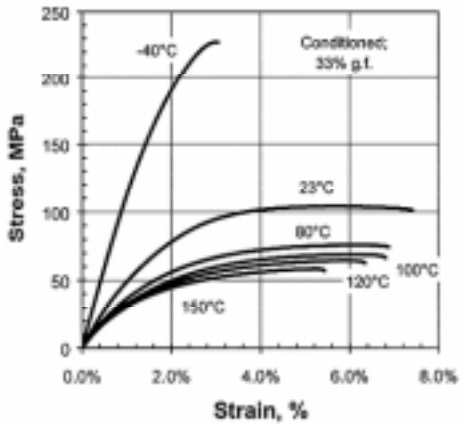


Figure 5b. Effect of temperature on tensile behavior of conditioned nylon 6 (33% glass fiber).

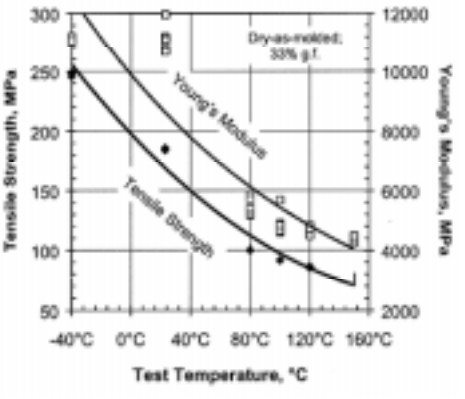


Figure 6. Effect of temperature on tensile strength and Young's modulus of dry-as-molded nylon 6 (33% glass fiber).

Although it has been well known that the moisture in thermoplastics will in general serve as a plasticizer that reduces a material's strength and increases its ductility, the current study indicates clearly that the net impact of moisture on tensile properties of nylon depends also on temperature. At –40°C, change in tensile behavior was insignificant within the elastic limit of the material (Figure 2a). About 10% decrease was found in the ultimate tensile

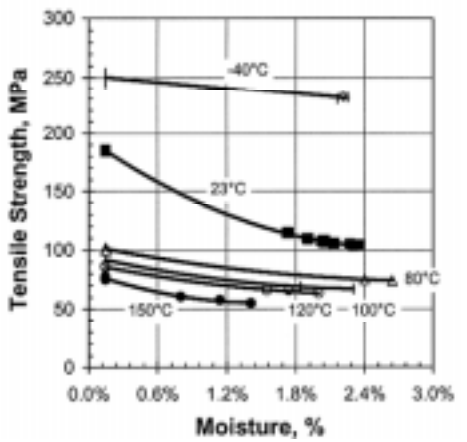


Figure 7. Impact of temperature and moisture on tensile strength of reinforced nylon 6 (33% glass fiber).

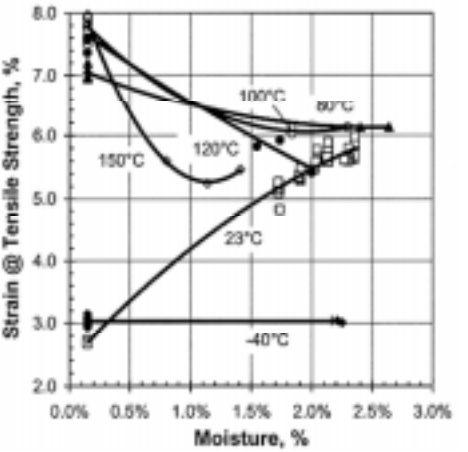


Figure 8. Impact of temperature and moisture on tensile strain @ tensile strength of reinforced nylon 6 (33% glass fiber).

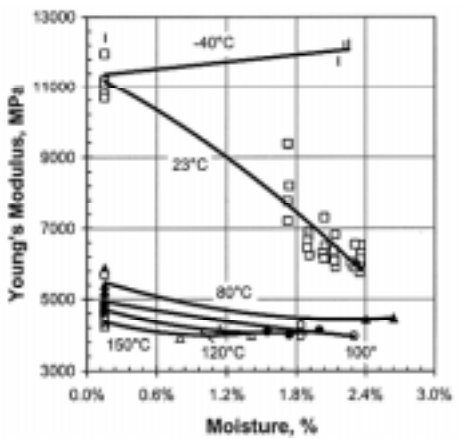


Figure 9. Impact of temperature and moisture on Young's modulus of reinforced nylon 6 (33% glass fiber).

strength after conditioning, but the total elongation (or strain) at failure remained virtually unchanged.

The most significant change in tensile behavior due to moisture can be found at room temperature where the tensile strength was reduced by about 40% after conditioning, while the elongation at failure increased by 150% (Figure 2b).

At elevated temperatures (80°C and above) where considerable plastic deformation in nylon has been resulted from heat, it was found that the conditioned samples exhibited not only a further reduction in strength, but lower overall elongation as well (Figure 2c).

Figures 2a to 5b seem to suggest that an increase in temperature or moisture can each achieve similar results in nylon, which is to reduce the material's strength and increase its ductility. However, the combination of temperature and moisture did not result in more ductility in the material that would allow it to deform further before failure. Instead, the material failed sooner with lower strength, indi-

cating that the high temperature and moisture together are able to cause deterioration in the reinforced nylon, and possibly other thermoplastic materials as well.

The tensile properties of nylon 6 at various temperature and moisture combinations are shown in Figures 7, 8, and 9. The values of these properties were obtained by measuring the moisture content in individual tensile bars immediately after each test using a Karl- Fischer analyzer described in Table 4. Each point on Figures 7 ~ 9 represents a single test. At each temperature (other than 23°C), the first test was conduced 1 hour after specimens were placed in the preheated chamber, and the subsequent tests were conduced approximately one every 20 minutes. One can see that, at each temperature, the tensile properties, especially the tensile strength and Young's modulus, correlate fairly well with the moisture measured individually from the test bars.

The results in Figures 7 ~ 9 also indicate that, in a hot and relatively dry environment, nylon can quickly lose its absorbed moisture, making the initial moisture level reported at the end of conditioning meaningless as a reference parameter to reflect the material's moisture state. The rise or fall in the material's properties (e.g., tensile parameters) following the change in temperature and relative humidity is something any design engineer must consider if he or she wishes to design and model structures or products made of thermoplastics.

## SUMMARY AND CONCLUSIONS

The individual and combined effects of temperature and moisture on the tensile properties of glass fiber reinforced nylon 6 were investigated and characterized. The sample conditioning was performed in an environmental chamber at 70°C and 62% RH as specified in ISO-1110. The conditioning was conducted until the moisture in the samples reached the equilibrium level under the standard conditions, i.e. 23°C/50%RH. The tensile property tests were conducted between –40°C and 150°C on ISO multipurpose test specimens with moisture levels from 0.2% (DAM) to 2.6% (conditioned). The following conclusions can be made as a result of the current investigation:

1. For nylon thermoplastics used in this investigation, both temperature and moisture can cause a decrease in strength and an increase in ductility. Among the selected temperatures, the moisture was found to cause the greatest change in tensile properties at 23°C. After conditioning, the material has lost 40% of its original tensile strength, and at the same time, the total elongation has increased by 150%.

2. At –40°C, nylon lost 10% of its tensile strength, but other characteristics such as tensile strain and Young's modulus remained largely unchanged, especially within the elastic limit.

3. At 80°C and above, the tensile strength and Young's modulus decreased further, while the elongation or strain to failure increased.

4. At elevated temperatures, the material properties have further deteriorated by adding moisture into the structure. Comparing to the dry-as-molded materials, the conditioned materials have lower tensile strength, and they also fail sooner.

5. Due to the rapid loss in moisture in a high temperature and low humidity environment, the initial moisture value obtained from a given nylon thermoplastic can quickly become meaningless once the material is exposed to such an environment. The rise or fall in the materials properties (e.g., tensile parameters) following the change in temperature and relative humidity is something one must consider in design, modeling, and manufacture of parts and products using moisture sensitive thermoplastics.

## ACKNOWLEDGMENT

The authors wish to express their sincere appreciation to Mr. Howard Fraenkel for the moisture conditioning and weight change measurement, and to Dr. Rich Williams for the moisture measurement using a Karl-Fischer unit.

## REFERENCES

1 N. Jia and V. A. Kagan, “Compatibility Analysis of Tensile Properties of Polyamides Using ASTM and ISO Testing Procedures”, SPE Annual Conference Proceedings / Antec’98, Vol.2, Materials, pp. 1706-1712, (1998).

2 N. Jia and V. A. Kagan, “Effects of Time and Temperature conditions on the Tensile-Tensile Behavior of Short Fiber Reinforced Polyamides”, SPE Annual Conference Proceedings / Antec’97, Vol. 2, pp. 1844-1848, (1997).

3 V. Kagan, “Good Vibrations Join Thermoplastics Fast”, *Machine Desig*n, August 5, 1999.

4 P. Bretz, R. Hertzberg, and J. Manson, “Influence of Absorbed Moisture on Fatigue Crack Propagation Behavior in Polyamides”, *Journal of Materials Scienc*e, vol. **16**, Part 1: Macroscopic Response, pp. 2061-2069, (1981).

5 N. Jia and V. A. Kagan, “Tensile Properties of Semi-Crystalline Thermoplastics – Performance Comparison under Alternative Testing Standards”, SAE Technical Paper Series, SAE International Annual Congress and Exposition, submitted to SAE’2000, Detroit (2000).

6 **Engineering Plastics**, Engineering Materials Handbook, Vol.2, *ASM International*, 883 pages, (1988).

7 M. Kohan, **Nylon Plastics Handbook**, *Hanser / Gardner Publications*, Inc., New York, 631 pages, (1995).

8 N. Rao and K. O’Brien, **Design Data for Plastics Engineers**, *Hanser / Gardner Publications, Inc.*, Cincinnati, 208 pages, (1998).

9 C. MacDermott and A. Shenoy., **Selecting Thermoplastics for Engineering Applications**, *Marcel Dekker, Inc*., New York, 305 pages, (1997).

# Temperature-Moisture-Mechanical Response of Vinyl Ester Resin and Pultruded Vinyl Ester/E-Glass Laminated Composites

**S. P. Phifer, K. N. E. Verghese, J. J. Lesko**
*Materials Response Group, Department of Engineering Science and Mechanics, Virginia Tech*
**J. Haramis**
*Department of Civil Engineering, Virginia Tech, Blacksburg, VA 24061-0219, USA*

## INTRODUCTION

High strength composite laminates are finding applications in infrastructure and construction industries. The high strength to weight ratio, corrosion resistance and durability are appealing, but the higher initial fabrication cost, in the past, has prevented composites from competing with products such as steel beams and wooden studs. With the advent of continuous pultrusion of constant cross-section laminated composites using low cost resin and fiber systems such as vinyl ester and E-glass, composites are successfully competing with these traditional materials. However, uncertainties in strength and durability of pultruded composites have hampered their wide-range use. Pultruded composites are similar to aerospace grade composites but differ in that the resins are more brittle, have higher shrinkage and less toughness. The fiber architecture is different due to the pultrusion requirement that all off-axis plies to the pultrusion direction must be attached to the on-pultrusion-axis plies. Only fiber aligned with the pultrusion axis can be pulled through the pultrusion die. Tricot stitching is generally used to attach off-axis plies to the on-axis plies which creates fiber bundles and gaps between the bundles. When the stitched plies are stacked to form a laminate fiber undulation and resin rich pockets are formed. With the high shrinkage resin, microcracking and delamination are plentiful in the as-processed condition. With fiber undulation, resin rich pockets, microcracking and delamination, pultruded laminates will potentially have lower strength, stiffness, moisture, temperature, and fatigue resistance than comparable aerospace grade composites.

E-glass fiber is known to degrade in moist environments due to an ionic exchange of the $H^+$ from the water with the metals such as sodium ($Na^+$),[1-4] which are loosely bound as

oxides in the silica. The resin acts to reduce the rate of degradation but matrix cracking, delamination, and exposed edges are sights for accelerating degradation.

The purpose of this research will be to experimentally obtain cross-ply, angle-ply, and resin strength and stiffness as a function of test temperature and time at elevated temperature immersion in tap water. Tensile and shear properties can then be determined to be used in specific application structural durability analysis.

## MATERIALS

### UNREINFORCED RESIN MATERIAL

The resin used to make samples for mechanical testing of the unreinforced polymer was Derakane™ 441-400 supplied by the Dow Chemical Company. The resin consists of a 690 g/mole, number average molecular weight oligomer and is diluted with 28% styrene in order to reduce its room temperature viscosity. The Derakane™ resin was cured with benzoyl peroxide (BPO), obtained from Aldrich. The material was 97% pure (lot # ES 03918CS). A BPO concentration of 1.1 wt% in Derakane™ was utilized (or a 0.011:1 ratio of BPO to Derakane). The resin was added to a suitable glass container. An Arrow 850 high torque stirrer was placed into the blend and stirring was set at the medium speed. The BPO was slowly added to the stirring mixture. After the BPO had dissolved (approximately 1 hour), the blend was degassed utilizing approximately 24 in Hg vacuum. The blend was allowed to degas for approximately 30 minutes. The catalyzed Derakane™ resin was cured utilizing the following procedure. An 20.34 cm x 15.24 cm x 0.635 cm vertical mold was utilized for the curing process to prevent the formation of air voids. The mold was treated with mold release and then assembled. The blend was added very slowly to the mold. After the top had been secured to the mold, it was then placed in a Fisher Isotemp forced convection oven. The material was cured utilizing the following cure cycle:
1 hour hold at 65°C → heating at 10°C/min to 150°C → 20 minute hold at 150°C.

The resin undergoes a rapid, free radically initiated addition copolymerization reaction to form the crosslinked network. After the mold had cooled to room temperature, the cured blend was removed. The samples were then cut on a water cooled circular table saw and then milled and ground to the required dimensions of 17.8 cm x 2 cm x 0.32 cm. In order to get the dog-bone geometry, the resin specimens were then placed in a fixture and hand fed through a four-fluted carbide end-mill attached to a router. The width of the gage section of the dog-bone is 1.27 cm in accordance with the ASTM D638-95 test standard.

### GLASS FIBER/VINYL ESTER COMPOSITE

The glass fiber reinforced composites were made using the Derakane™ 411-350 vinyl ester resin that was supplied by the Dow Chemical Company. The E glass fiber was obtained

from Owens Corning and the lay up is [One, Nexus NS veil cloth/One, CDM "1810" C, 0/90°/continuous strand mat complex/Two, CD 185, 0/90° stitched mats]$_S$. The composites were made using pultrusion in the Dow facility at Freeport, Texas. The width of the die used was 18 cm. The pultrudable grade of Derakane$^{TM}$ 411-350 consists of fillers such as calcium carbonate, UV stabilizer, air release agent and mold release agent. A proprietary initiator package was used to cure the vinyl ester using a free radical mechanism similar to the one explained above. During pultrusion both the pull force and die temperature were monitored at all times. Die temperatures were measured at the entrance, midpoint, and exit using thermocouples. For the vinyl ester laminates, die temperatures were set at 240°F, 280°F, and 280°F, respectively. A pull speed of around 45 cm/minute was used and pieces 54 cm long were cut periodically using a tabletop circular saw. The final test specimen dimensions of 17.8 cm x 2.54 cm x 0.4 cm were achieved by using a water-cooled circular saw. The edges of the specimens were not sealed but were polished using 100, then 400, followed with 600 grit wet sandpaper.

## EXPERIMENTAL PROCEDURE

Tensile tests were performed in accordance with ASTM D3039-95a, and D3518-95 for the cross-ply and angle-ply (±45°) composites respectively and ASTM D638-95 for the resin in dog-bone form. These tests were performed using an Instron test frame operated in displacement control at a rate of 1.25 mm/min. Both extensometers and strain gages were used to measure strain. In the case of the resin samples, the aluminum extensometer tabs and strain gages were found to induce failure at those sites when tested at room temperature and below. Use of silicone extensometer tabs alleviated this problem.

## RESULTS AND DISCUSSION

### UN-AGED (AS RECEIVED) MATERIAL

#### Mechanical Properties

Unaged properties of the resin, cross-ply and angle-ply laminates are shown in Table 1. Error bars in the figures represent ± 1 standard deviation. Typical stress-strain plots, normalized by ultimate strength, are also indicated in Figure 1 to present the plasticity of the resin and angle-ply specimens at room temperature.

#### Test Temperature Effects

In order to evaluate the effects of temperature on mechanical properties of these materials, tensile tests were performed at temperatures ranging from –50°C to 90°C. A comparison of the tensile strength and stiffness was made for the resin, cross-ply and angle-ply laminates. The room temperature tensile strength data, normalized to room temperature ultimate

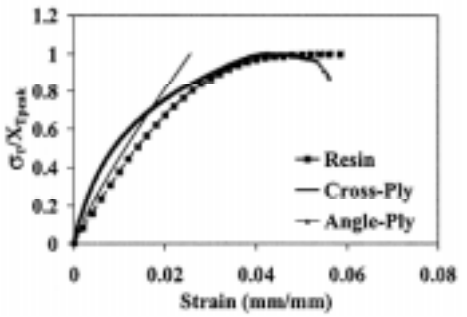


Figure 1. Tensile stress/strain curves normalized to peak tensile strength.

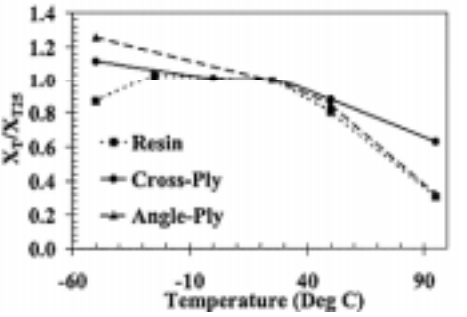


Figure 2. Tensile strength normalized to room temperature unaged tensile strength.

strength, showed that the resin and angle-ply follow the same curve from 0°C to 95°C, Figure 2. However, a peak near -25°C is seen to exist for the resin. This is speculated to be due to the increasingly brittle nature of the resin that makes it extremely notch sensitive at sub-ambient temperatures. On the other hand, the angle-ply laminates, withstand substantial microcracking, permitted higher strength at sub-ambient conditions. At 95°C the strengths of both angle-ply and cross-ply laminates were seen to monotonically decrease to 60% and 30% respectively of their room temperature, unaged strengths. The tensile modulus of the resin and shear modulus of the laminate reduced monotonically with increased temperature. The tensile modulus of the laminate on the other hand was seen to be constant from -50°C to 25°C after which it decreased monotonically, Figure 3.

**Table1. Unaged 25°C mechanical tensile properties with standard deviation**

| Specimen | Tensile modulus, GPa (Msi) | Ultimate strength, MPa (Ksi) | Strain at ultimate strength (mm/mm) |
|---|---|---|---|
| Resin | 3.32±0.05(0.48±0.01) | 82.6±1.0(12.0±0.1) | 4.85±0.59 |
| Angle-ply | 3.71±0.23(0.54±0.03) | 55.8±1.3(8.1±0.2) | 4.41±0.26 |
| Cross-ply | 23.9±3.4(3.47±0.50) | 431±12(62.5±1.8) | 2.58±0.35 |

## ENVIRONMENTALLY AGED MATERIAL

### Moisture Absorption

Samples were immersed in water at 45°C and 80°C. Although from previous studies performed by the authors the resin was observed to follow a Fickian uptake behavior when

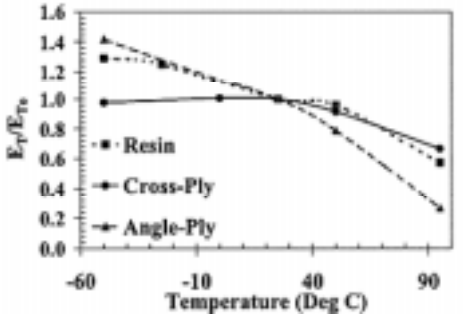


Figure 3. Tensile modulus normalized to room temperature unaged modulus

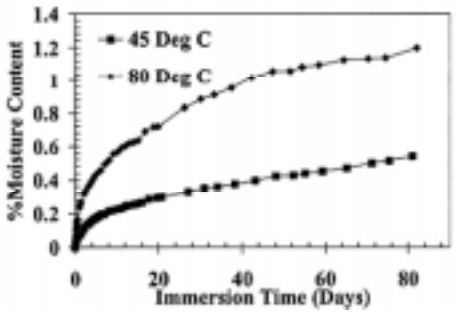


Figure 4. Pultruded vinyl ester E-glass laminate % moisture content (MC) verses time of immersion.

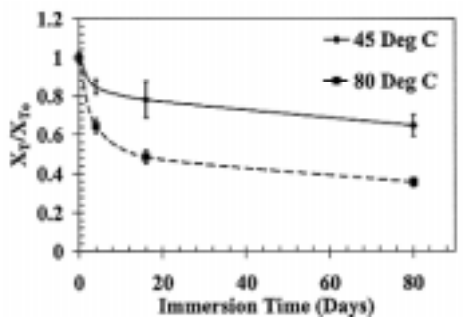


Figure 5. Cross-ply tensile strength normalized to unaged 25°C strength verses time of immersion.

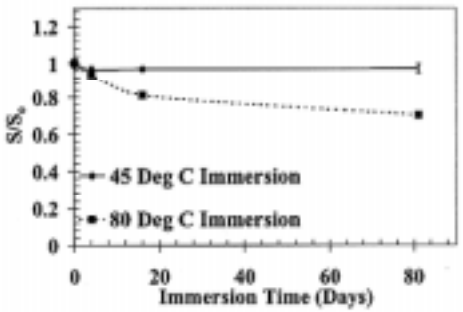


Figure 6. Angle-ply shear strength normalized to unaged 25°C shear strength verses time of immersion.

immersed in water at 80°C with an equilibrium moisture content of 1.1%, large deviations were noticed for the composite. Therefore the experiment was arbitrarily terminated after 80 days at which point the moisture contents were 0.5% and 1.2% by weight respectively. Figure 4 shows the uptake plots at both 45°C and 80°C for the cross ply laminate. Others[5-7] have shown that the equilibrium moisture content in similar vinyl ester/E-glass composites should be reached within approximately 10-12 days in 93 and 80°C temperature water immersion. In the present case from a simple rule of mixtures approach, it is clear that this is higher than the moisture content for the resin by itself when normalized to percent resin content of 37% in the composite. The E-glass fiber, interface, matrix cracks, and delaminations are speculated to be influencing the moisture absorption rate and equilibrium value. The degradation is therefore both a function of temperature and time.

### Mechanical Properties (Immersion Aging Time Effect):

In order to assess the effects of time of exposure on the mechanical property retention, cross-ply and angle-ply laminate specimens were aged for 4, 16, and 80 days in 45°C and 80°C temperature water. Tensile tests were then performed at room temperature. This non-fickian moisture absorption behavior mirrors the trend of cross-ply tensile strength reduction with immersion time, as shown in Figure 5. For the cross-ply laminate, immersion for 4 days in 45°C and 80°C water, the strength was reduced to 85% and 65% respectively when compared to the room temperature, as-fabricated strength. Prolonged immersion for 80 days further reduces the strength to 65% and 35%. The modulus of the cross-ply laminate reduces to 95% and 85% with immersion of 80 days in 45°C and 85°C water respectively.

Experimental observation of the failure mechanism for the cross-ply laminate revealed changes from the unaged to aged material. A sudden event marked the failure of the unaged and 80 day aged cross-ply specimens. The failure of the 4 and 16 day aged cross-ply specimens began with a few loud pops followed by a continuous popping over 5 to 15 seconds. The stress strain curves for the 4 and 16 day aged specimens therefore became nonlinear near end of life due to this slow failure sequence.

The shear response measured from the angle-ply laminate is less affected by immersion in 45°C and 85°C water (Figure 6). Immersion of 4 days reduces the shear strength to 95% and 93% respectively, and immersion of 80 days reduces the strength to 95% and 70% respectively. Shear modulus, not shown in the figures, is little effected by immersion aging.

### Mechanical Properties (Test Temperature Effects)

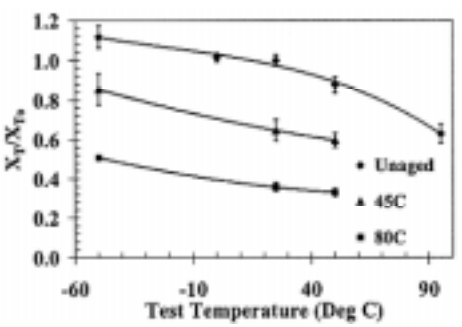


Figure 7. Comparison cross-ply tensile strength relative to test temperature for specimens unaged and immersed for 80 days in 45°C and 80°C water.

Cross-ply and angle-ply laminate specimens, immersed in 45°C and 80°C temperature water for 80 days, were tensile tested at –50°C, 25°C and 50°C. The aged, cross-ply specimens, Figure 7, had nearly parallel strength/temperature curves to the unaged but were reduced by 35% and 65% for 45°C and 80°C/80 days aging respectively. The shear strength of the angle-ply, Figure 8, is not reduced at 45°C/80 day immersion but at 80°C/80 days immersion the shear strength/temperature curve is parallel to the unaged composite but is offset by 25-30%. The tensile modulus of the cross-ply laminate aged at 45°C for 80 days showed little difference when compared to the unaged material (Figure 9). When this was compared to the changes in shear modulus of the aged angle-ply laminates, despite the overall test temperature related trends, little or no change was noticed as a func-

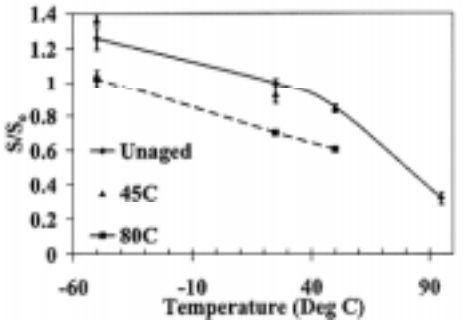


Figure 8. Comparison angle-ply shear strength relative to test temperature for specimens unaged and immersed for 80 days in 45°C and 80°C water.

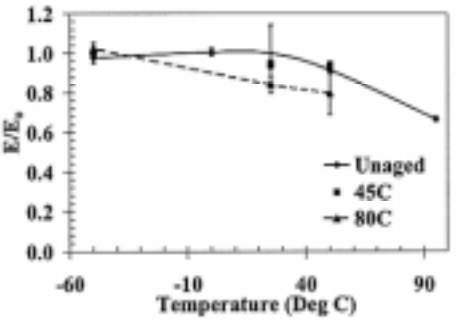


Figure 9. Comparison cross-ply tensile modulus relative to test temperature for specimens unaged and immersed for 80 days in 45°C and 80°C water.

tion of aging conditions. All of the above mentioned trends indicate that the properties of the matrix polymer is not affected by hygrothermal aging and is only affected by test temperature. The E-glass reinforcement however is extremely sensitive to both temperature and moisture.

## CONCLUSIONS

The tensile and shear strength of the cross-ply and angle-ply monotonically decreased with increasing temperature over the range of –50 to 95°C. In contrast, the resin tensile strength peaked near -25°C.

The Derakene 411-400 resin had a Fickian moisture uptake when immersed in 80°C water. The vinyl ester/E-glass composites exceeded the resin equilibrium moisture content when normalized with resin content of the composite and did not reach equilibrium within the 80-day immersion period in 45, 65, or 80°C temperature water. The fiber dominated tensile strength of the cross-ply laminate after immersion, decreased rapidly initially. In 14 days the cross-ply tensile strength was reduced to 78% and 48% for 45°C and 80°C immersion temperatures respectively; while only an additional 12% and 15% reduction was noted from 14 to 80 days of immersion respectively. From the data obtained at different test temperatures on hygrothermally aged specimens it was noticed that the resin was affected primarily by temperature and not aging condition while the glass fiber was sensitive to both water as well as temperature. Visible discoloration was noticed on the samples that were immersed in water. The rate of discoloration was seen to be a function of both aging temperature as well as aging time. Failure surfaces of samples tested after saturation indicated that this discoloration was limited to the outer layers of the composite even after 80 days in 80°C water. It was speculated that damage (debonding) to the surface veil cloth as well as outer

ply fibers was responsible for this discoloration. Preliminary scanning electron microscopy (SEM) work indicated the formation of cracks around the several fibers on samples exposed to 80°C water. The progression of these cracks both in terms of magnitude and position relative to the surface plies seems to be dependent on the length of exposure.

## FUTURE WORK

Tensile testing of the unreinforced resin after saturation in water at 45°C and 65°C will be necessary, in order to better understand the hygrothermal response of the polymer. To complete the study on the effects of aging time on property retention, 4, 16 and 80-day aging tests at 65°C for the cross-ply laminate will be performed. Similar tests will also be carried out at additional temperatures of 20°C and 35°C to ascertain the thermal dependence of the rate of strength reduction. The goal will be to devise a.scheme to calculate a characteristic time for degradation and the activation energy for the process, similar to ideas presented by Phani and Bose.[8]

## ACKNOWLEDGEMENTS

The authors wish to thank Dr. P. M. Puckett, Herbert Englen of The Dow Chemical Company, Freeport, Texas and Timothy MacNeil of Owens Corning for supplying the materials and pultrusion facilities. The authors also express their gratitude to Dr. D. A. Dillard at Virginia Tech for time on the Instron.

## REFERENCES

1 Charles R. J., *Journal of Applied Physics*, **29**:11 1549-1560 (1958).
2 Metcalfe A. G. and G. K.Schmitz, *Glass Technology* **13**:1 5-16 (1972).
3 Bank L. C., T. R. Gentry, and A. Barkatt, *Journal of Reinforced Plastics and Composites*, **14** 559-587 (1995).
4 Schultheisz, C. R. et al. *ASTM STP 1242*, 257-286 (1997).
5 Springer G. S., **Environmental Effects on Composite Materials**, Volume 2 59-78 (1984).
6 Springer G. S., *Journal of Composite Materials*, **14** 213-232 (1980).
7 Sridharan S, A. H. Zureick, and J. D. Muzzy, ANTEC'98, 2255-2259 (1998).
8 Phani K. K, N. R. Bose, *Composites Science and Technology*, **29**, 79-87, (1987).

# Freeze-thaw Durability of Composites for Civil Infrastructure

**J. Haramis**
*Department of Civil Engineering, Virginia Tech*
**K.N.E. Verghese, J. J. Lesko**
*Materials Response Group, Department of Engineering Science and Mechanics, Virginia Tech, Blacksburg, VA 24061, USA*

## INTRODUCTION

Fiber reinforced polymer (FRP) composite materials are under consideration for use in civil infrastructure within the U.S. primarily due to their high strength and stiffness to weight ratios and their design flexibility for specific structural characteristics. In addition, the serviceability and functional service life of a composite structure such as a bridge may be greater than those built using conventional structural materials. One uncertainty that hampers attempts to routinely implement FRP in highway structures is proof of environmental durability. As of today a comprehensive database of information does not exist nor does a fundamental understanding of the physics of the problem at hand.

Freeze-thaw durability is one such environmental condition that is not well understood. Limited research has been conducted in this area but it is typically targeted to aerospace applications.[1]

Work targeted specifically to civil infrastructure applications by Gomez and Casto[2] has reported mechanical data on freeze-thaw tests conducted on isophthalic polyester and vinylester pultruded glass reinforced composites. Specimens were aged in accordance with ASTM C666 (namely, 40°F to 0°F followed by a hold at 0°F and a ramp up to 40°F followed by a hold) while submerged in 2% sodium chloride and water. Specimens were removed after every 50 cycles and tested in flexure mode. The results clearly indicated a reduction in flexure strength and modulus after 300 cycles.

Lord and Dutta[3] were, according to the authors, one of the first to highlight the importance of cracks in the matrix and fiber-matrix interface as being the cause of the damage in composite materials. When these cracks form beyond a certain critical size and density they coalesce to form macroscopic matrix cracks which tends to increase the diffusion of water into the system. Water can then condense within these cracks resulting in crack propagation

as well the formation of micro and macro level ply delamination during the expansion of water undergoing a liquid-solid phase transition.

In Kevlar fabric laminates used by Allred[4] subjected to two hour temperature cycles from –20°F to 125°F, ultimate tensile strength of the laminate was found to decrease by 23% after 360 cycles and by 63% after 1170 cycles.

In work by Verghese, et al.[5] differential scanning calorimetry (DSC) was used to identify the nature and presence of freezable water for each constituent material within an E-glass/vinylester composite, i.e., matrix, and interphase (via an assembled composite). Thawing heat flow measurements taken for a single cycle (-150°C to +50°C, 5°C/min) on saturated, neat, unreinforced vinylester resin samples indicated no thawing endotherm and thus the absence of freezable water. This was attributed to the fact that water would reside in the free volume of the resin. Since this free volume size is on the order of about 6-20 Å, Thompson's equation indicates that these voids will be thermodynamically too small for water to freeze. Heat flow measurements taken for an E-glass/ vinylester composite with the same cycle parameters clearly indicated a melt endotherm at –6.8ºC thus indicating the presence of small voids at the interphase region within the composite and potential susceptibility to freeze-thaw degradation. Cyclic DSC cycling (–18°C to +4°C, 5°C/min) of an E-glass/ vinylester composite displayed a shift up in the thaw endotherm as cycling progressed, indicative of freeze-thaw damage via increased void size.

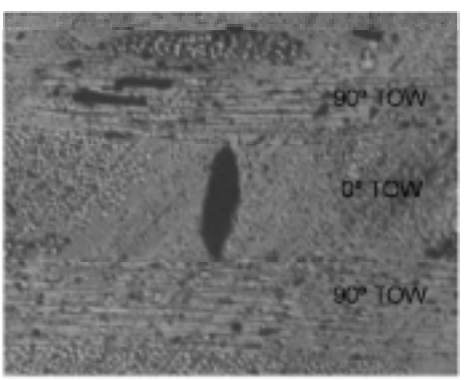


Figure 1. Typical crack in toughened vinylester composite (0.24mm by 0.08mm).

It seems unlikely that water can freeze in limited void system of a neat polymer resin, but the crack dimensions in a composite system appear are large enough to facilitate the freezability of water (see Figure 1). Work is underway to understand the effects of moisture and freeze-thaw on residual mechanical properties of $[0°/90°]_{3s}$, glass/ vinylester and glass/epoxy composites. This work will help further our understanding of the effects of different environmental conditions, in particular, freeze-thaw.

## EXPERIMENTAL PROCEDURE

### OVERVIEW

Both saturated and dry fiber reinforced polymeric composite samples will be placed in an accelerated freeze-thaw environment and tested for mechanical property degradation, changes in crack density, and moisture uptake at specified intervals to assess damage. A group of saturated controls will be held at a constant temperature above freezing and will be

tested in the same manner as the freeze-thaw samples. All samples are pultruded glass reinforced cross-ply (0/90) laminates with polymeric matrix materials.

## MATERIALS

All materials were pultruded using an open resin impregnation bath. During pultrusion both pull force and die temperature were monitored at all times and allowed to reach steady state before any material was considered usable.

Three different matrix resins were used in this study: a toughened vinyl ester, an untoughened vinyl ester, and an epoxy. Two different fiber lay-ups were used designated by the letters “L” and “P”. The vinylester laminates were pultruded with the “L” lay-up while the epoxy laminate employed the “P” lay-up in order to prevent scaling problems in the epoxy resin system. Tables 1 and 2 detail the two lay-ups.

**Table 1. Fiber Lay-up “L”**

| | |
|---|---|
| Reinforcement #1 | 2 x XCDM 1810 “C” Complex |
| Reinforcement #2 | 4 x CD 185 Complex |
| Surface veil | 2 x Nexus 039 |

**Table 2. Fiber Lay-up “P”**

| | |
|---|---|
| Reinforcement #1 | 2 x XCDM 1810 “C” Complex |
| Reinforcement #2 | 4 x CD 185 Complex |
| Reinforcement #3 | 1 x 300 g/m$^2$ (1.0 ox) M8643 |
| Surface veil | 2 x Nexus 039 |

From the batch of pultruded material, 510 samples were cut to 25.4 mm by 177.8 mm (1 inch by 7 inches) from the larger as-received panels using an abrasive wet saw. Special care was taken to align all saw cuts with the principal material directions with the long direction corresponding to pull direction. All laminates were nominally 4 mm (0.160 inches) thick. After the cutting operation, the edges of each sample were wet sanded smooth with 400-grit abrasive paper and blown dry with compressed air. All samples destined for saturation were edge coated with an oven cured two-part epoxy to prevent moisture infusion through cut edges.

## AS-RECEIVED TESTING AND ANALYSIS

Ultimate tensile strength, stiffness, and strain-to-failure were determined quasi-statically for each class of as-received material in accordance with ASTM D 3039 “Standard Test Method

for Tensile Properties of Polymer Matrix Composite Materials" using a deflection rate of 2.5 mm/min (0.10 inches/min). A total of thirty samples were tested, ten of each material type. In addition, two samples of each material were set aside for crack density analysis using x-ray and optical microscopy techniques.

## SATURATION AND MOISTURE UPTAKE ANALYSIS

324 samples were fully saturated in a 65°C (149°F) water bath with moisture uptake measured throughout the saturation process. Weight measurements were taken hourly on the first day the samples were placed in the saturation tank, every three hours on the second day, every four hours the third day, every six hours the fourth day, and once everyday thereafter. The samples reached saturation within 45 days.

## FREEZE-THAW CONDITIONING

Figure 2. Freeze-thaw conditioning chamber.

The freeze-thaw conditioning parameters chosen for this research study were based on ASTM C 666 "Standard Test Method for Resistance of Concrete to Rapid Freezing and Thawing". This test protocol calls for a ramp down from 4.4°C (40°F) to -17.8°C (0°F) followed by a hold at -17.8°C (0°F), a ramp up to 4.4°C (40°F) and a hold at -17.8°C (0°F). There may be a minimum of 4.8 and a maximum of 12 conditioning cycles per day with 75% of the cycle time set aside for freezing and 25% for thawing. Two high performance cascading refrigeration freeze-thaw conditioning chambers (see Figure 2) will be used to achieve a ten cycle per day rate.

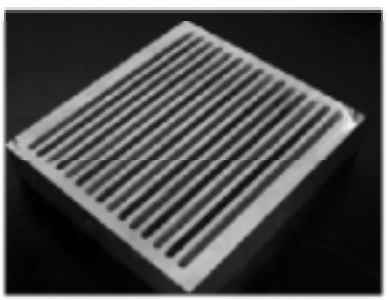

Figure 3. Unloaded sample freeze-thaw tray.

A series of trays was fabricated to hold each sample in accordance with ASTM C 666, namely to surround the samples with between 0.8 mm (1/32 inch) to 3.2mm (1/8 inch) of water. Additional design goals for the trays were to minimize the volume of water and maximize convective heat transfer with the air inside chamber. A finished tray is shown in Figure 3. Each tray can hold eight samples and every other slot was machined all the way through to allow airflow vertically through the trays.

Figure 4. Loaded sample freeze-thaw tray.

A second type of tray was also fabricated to allow the application of four point bending loads to each sample capable of causing 0.55% strain at the centerline on the surface of the tension face, see Figure 4. This strain level was chosen because it is beyond the “knee” in the stress-strain curve for each material in this research study and it likely opens up cracks that might be large enough to allow additional freezing to take place. This tray can also hold up to eight samples.

Three levels of freeze-thaw exposure will be included in this study: 100, 300, and 500 cycles. A set of control samples will also be placed in a constant 4.4°C (40°F) bath for the duration of each freeze-thaw exposure level.

## POST-CONDITIONING TESTING AND ANALYSIS

Similar to the as-received testing regime, ultimate tensile strength, stiffness, and strain-to-failure were determined quasi-statically in accordance with ASTM D 3039 for each class of material after saturation. A total of thirty samples were tested, ten of each material type. In addition, two samples of each material were set aside for crack density analysis using x-ray and optical microscopy techniques.

Similar mechanical testing and crack density analyses will be performed at each of the three specified freeze-thaw conditioning levels for both unloaded and loaded samples in each of the general conditioning categories, i.e., saturated freeze-thaw (144 samples), saturated constant temperature (144 samples), and dry freeze-thaw (144 samples).

## CRACK DENSITY ANALYSIS

Crack density was/will be assessed using non-destructive acousto-ultrasonic (AU) techniques with confirmation by optical microscopy.

AU is an ultrasonic NDE technique useful for quantifying small, distributed changes not easily detected with traditional ultrasonic techniques. It returns results related to the ability of the interrogated material to transfer mechanical energy. In this setup, the transducers are spaced in a manner (typically, far apart) so that there is no direct or minimally reflected energy transmission between them and the primary transmission is by plate wave propagation. AU results are calculated from the energy spectral distribution of the AU signal by moment analysis. The most useful AU parameters tend to be the area under the curve (zeroth order moment) and the centroidal frequency (ratio of the first and zeroth moments). The area is directly related to the amount of energy transfer along the specimen. Shifts in the

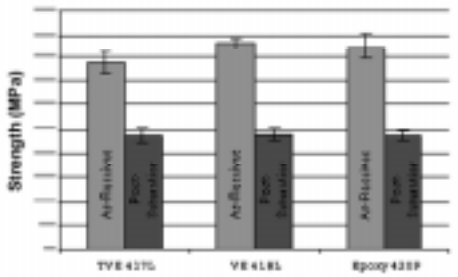


Figure 5. As-received and post-saturation strength data.

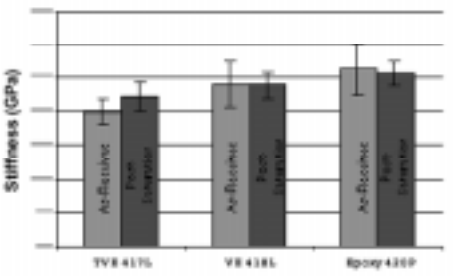


Figure 6. As-received and post-saturation stiffness data.

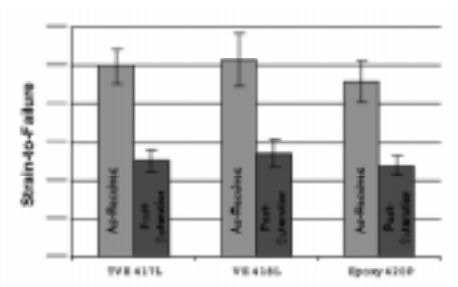


Figure 7. As-received and post-saturation strain-to-failure data.

centroidal frequency also indicate changes in the materials ability to propagate particular modes. Typically, the spectral content of the AU signal has several relatively discrete frequency peaks with a few dominant ones. Each peak corresponds to a different mode or order of plate wave propagation. The modes are typically categorized as symmetric (extensional) and antisymemetric (flexural). The order of a particular mode indicates the complexity of that type of deformation. Since each peak represents energy propagating with a different type of deformation, it possibly can be sensitive to different types of degradation. AU samples will be taken from the general sample population and have already been baselined for as-received and post-saturation conditions.

For optical microscopy, representative sections of material will be cut, potted, and polished for each post-conditioning group and examined using an inverted optical microscope.

## RESULTS

Though this research is still in its early stages, some data can be reported. Tensile strength, stiffness, and strain-to-failure are shown in Figures 5 through 7.

Strength for the toughened vinylester was 389 MPa in the as-received condition versus 237 MPa for the post-saturation condition. Likewise, for the untoughened vinylester, strengths were 432 MPa versus 240 MPa. For the epoxy, strengths were 424 MPa versus 237 MPa.

Stiffness for the toughened vinylester was 19.9 GPa in the as-received state versus 22.1 GPa for the post-saturation condition. Stiffness for the untoughened vinylester, was 23.9

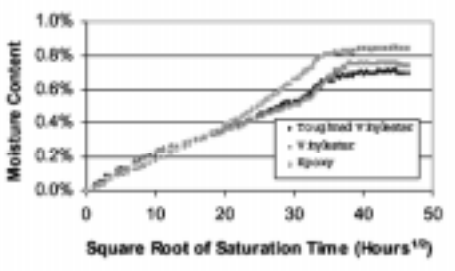


Figure 8. Moisture uptake curves for saturation at 65ºC.

GPa for both conditions. For the epoxy, stiffness was 26.2 GPa versus 25.6 GPa.

Strain-to-failure for the toughened vinylester was 2.49% in the as-received condition versus 1.26% for the post-saturation condition. For the untoughened vinylester, strain-to-failure was 2.58% versus 1.36% and for the epoxy, 2.29% versus 1.20%.

In summary, strength and strain-to-failure were approximately 50% lower after saturation for all three materials. Stiffness effectively remained unchanged. The moisture content at saturation was 0.70% for the toughened vinylester samples, 0.74% for the untoughened vinylester samples, and 0.84% for the epoxy samples. A moisture uptake curve is presented in Figure 8. It is clear from the curves that the composite does not obey Fick's law. Because of this, the moisture aging experiment had to be terminated after 45 days at which point the heaters were turned off and the tank was allowed to equilibrate to room temperature.

## CONCLUSIONS AND FUTURE WORK

It is virtually impossible to freeze water in a highly crosslinked amorphous polymer. This is in part due to geometric space constraints in addition to hydrogen bonding that further impedes the process. In the composite system however, the crack dimensions are large enough to facilitate the freezability of water. The authors believe that this is this mechanism of freezing and the associated volume increase during the transition leads to the propagation of cracks and the accumulation of damage.

Work is underway to begin freeze-thaw cycling and damage assessment as discussed earlier in this paper. It is hoped that information regarding crack density will be used to better understand the trends in strength and stiffness of these composites and the effect on freeze-thaw durability.

## ACKNOWLEDGMENTS

The authors would like to thank Dow Chemical Corporation, Dr. P. M. Puckett, and Herbert Englen for the use of their facilities and personnel in the pultrusion activities related to this research as well as their donation of the various resin systems. The authors would also like to thank Tim MacNeil and Owens-Corning for their donation of the glass reinforcement complexes used in this research.

## REFERENCES

1 Mitra, Dutta and Hansen, “Thermal Cycling Studies of a Cross-plied P100 Graphite Fiber Reinforced 6061 Aluminum Composite Laminate”, *Journal of Materials Scienc*e, 26, November 1991.

2 Gomez, J. P. and Casto, B., “Freeze-Thaw Durability of Composite Materials”, Virginia Transportation Research Council, 1996.

3 Lord, H. W., and Dutta, P. K, “On the Design of Polymeric Composite Structures for Cold Regions Applications”, *Journal of Reinforced Plastics and Composite*s, 7, 1988.

4 Allred, R. E., “The Effects of Temperature and Moisture Content on the Flexural Response of Kevlar/Epoxy Laminates: Part II [45/0/90] Filament Orientation”, **Environmental Effects on Composite Materials**, Volume 2, George Springer, editor, Lancaster, PA: *Technomic Publishing Company, Inc*., 1984

5 Verghese, N., Haramis, J. Morrell, M.R., Horne, M.R., and Lesko, J.J. “Freeze-Thaw Durability of Polymer Matrix Composites in Infrastructure”, To be published in the proceedings of Duracosys’99.